Cell Wall Invertase Is Essential for Ovule Development through Sugar Signaling Rather Than Provision of Carbon Nutrients[1][OPEN]

Shengjin Liao, Lu Wang, Jun Li, and Yong-Ling Ruan[2,3]

School of Environmental and Life Sciences and Australia-China Research Centre for Crop Science, The University of Newcastle, Callaghan, New South Wales 2308, Australia

ORCID IDs: 0000-0003-4064-7610 (L.W.); 0000-0002-8394-4474 (Y.-L.R.).

Ovule formation is essential for realizing crop yield because it determines seed number. The underlying molecular mechanism, however, remains elusive. Here, we show that cell wall invertase (CWIN) functions as a positive regulator of ovule initiation in Arabidopsis (*Arabidopsis thaliana*). In situ hybridization revealed that *CWIN2* and *CWIN4* were expressed at the placenta region where ovule primordia initiated. Specific silencing of *CWIN2* and *CWIN4* using targeted artificial microRNA driven by an ovule-specific SEEDSTICK promoter (*pSTK*) resulted in a substantial reduction of CWIN transcript and activity, which blocked ovule initiation and aggravated ovule abortion. There was no induction of carbon (C) starvation genes in the transgenic lines, and supplementing newly forming floral buds with extra C failed to recover the ovule phenotype. This indicates that suppression of CWIN did not lead to C starvation. A group of hexose transporters was downregulated in the transgenic plants. Among them, two representative ones were spatially coexpressed with *CWIN2* and *CWIN4*, suggesting a coupling between CWIN and hexose transporters for ovule initiation. RNA-sequencing analysis identified differentially expressed genes encoding putative extracellular receptor-like kinases, MADS-box transcription factors, including *STK*, and early auxin response genes in response to CWIN-silencing. Our data demonstrate the essential role of CWIN in ovule initiation, which is most likely to occur through sugar signaling instead of C nutrient contribution. We propose that CWIN-mediated sugar signaling may be perceived by, and transmitted through, hexose transporters or receptor-like kinases to regulate ovule formation by modulating downstream auxin signaling and MADS-box transcription factors.

In higher plants, most carbohydrate making up the bulk of the biomass and crop yield originates from Suc, making Suc a crucial yield determinant (Ruan, 2014). Suc is predominately derived from photosynthetically active leaves and translocated through phloem to sink organs. Upon being delivered to sinks, it is degraded either by Suc synthase (Sus; EC 2.4.1.13) or invertase (INV; EC 3.2.1.26). Sus reversibly degrades Suc into uridine diphosphate (UDP)-Glc and Fru in the presence of UDP. INV, on the other hand, irreversibly hydrolyzes Suc into Glc and Fru. Based on their subcellular location, INVs are classified into three subgroups: cell wall invertase (CWIN), vacuolar invertase (VIN), and the structurally unrelated cytoplasmic invertase (CIN; Sturm, 1999, Wan et al., 2018). CWINs, also referred to as extracellular or apoplasmic INVs, are insoluble proteins ionically bound to the cell wall with a pH optimum of 3.5 to 5.0 (Roitsch and González, 2004). Although symplasmic transport through plasmodesmata (PDs) is considered a common pathway for Suc unloading, Suc can only be transported apoplasmically across cell wall matrix and plasma membranes in cellular interfaces lacking the PD connection (Patrick, 1997). In the latter case, Suc is often unloaded from the sieve element-companion cell (SE/CC) to the surrounding cell wall matrix, and then taken up by recipient sink cells via Suc transporters (SUTs) or hexose transporters (HXTs) following hydrolysis of Suc by CWIN at the extracellular space (Braun et al., 2014; Li et al., 2017).

The CWIN-SUT/HXT nexus could also operate in regions beyond the SE/CC unloading site for post-phloem delivery of assimilates in sink organs (Li et al., 2017). For example, as a common feature of all developing angiosperm seeds, the filial tissue (endosperm and embryo) is symplasmically isolated from the surrounding maternal seed coat or pedicel in dicot or monocot species, respectively. In this scenario, assimilates must be transported across the apoplasmic compartment between the maternal and filial tissues to nurture the developing embryo, where CWIN could play a critical role in seed development (Patrick 1997; Weber et al., 2005). A classic example is the maize (*Zea mays*) miniature-seed

[1]This work was supported by the Australian Research Council (grant no. DP180103834).

[2]Senior author.

[3]Author for contact: yong-ling.ruan@newcastle.edu.au.

The author responsible for distribution of materials integral to the findings presented in this article in accordance with the Journal policy described in the Instructions for Authors (http://www.plantphysiol.org) is: Yong-Ling Ruan (yong-ling.ruan@newcastle.edu.au).

Y.L.R. conceived the project; Y.L.R. and L.W. supervised the work; S.J.L. and J.L. performed the experiments; S.J.L., L.W., and Y.L.R. analyzed the data; S.J.L. and Y.L.R. wrote the article.

[OPEN]Articles can be viewed without a subscription.

www.plantphysiol.org/cgi/doi/10.1104/pp.20.00400

phenotype as a result of mutation of a CWIN gene expressed in the endosperm transfer cell, the outermost cell layer of the filial tissue facing the pedicel (Miller and Chourey, 1992). Similarly, in fava bean (*Vicia faba*), CWIN activity at the innermost layer of the seed coat positively correlates with cell division of cotyledons, hence seed size (Weber et al., 1996). In developing tomato fruit (*Solanum lycopersicum*), a CWIN gene is mainly expressed in the phloem of placenta connecting the developing seed where unloading occurs apoplasmically (Jin et al., 2009; Palmer et al., 2015). Here, genetically elevating the endogenous CWIN activity increased seed weight (Jin et al., 2009), whereas silencing its expression resulted in stunted seed (Zanor et al., 2009). A similar role for CWIN has been reported in other species, including rice (*Oryza sativa*; Wang et al., 2008) and barley (*Hordeum vulgare*; Weschke et al., 2003).

Apart from its function in Suc unloading, CWIN also plays a role in sugar signaling (Ruan, 2012). For instance, the maize miniature seed phenotype of CWIN-deficient mutant could not be recovered by the provision of exogenous hexose (Cheng and Chourey, 1999), and enhancing *CWIN* expression in the shoot apical meristem accelerated flowering and increased inflorescence branching in Arabidopsis (*Arabidopsis thaliana*; Heyer et al., 2004). More recently, elevation of CWIN activity in tomato was found to induce the expression of R and PR genes in fruitlets (Ru et al., 2017) and to block programmed cell death under heat stress (Liu et al., 2016). These findings indicate that CWIN has a signaling function in development and defense, but they do not differentiate between that and its role in providing sugar nutrients.

Despite the extensive studies of CWIN as outlined above, it remains unknown whether and how CWIN may exert its potential role in the formation of seed precursors, ovules, at the prefertilization stage. Ovule initiation and establishment represent a crucial window that sets yield potential, as ovule formation determines seed number. Not only would progress on this frontier contribute to our understanding of the roles of CWIN-mediated Suc metabolism or signaling in prefertilization reproductive development, it could also uncover promising targets for designing innovative approaches to enhance crop seed yield.

In this study, we reported that two CWIN genes, *CWIN2* and *CWIN4*, were highly expressed in the placenta region of gynoecia where ovule primordia initiate. To determine their potential role in ovule development, we generated transgenic lines in which an ovule-specific *SEEDSTICK* promoter (*pSTK*; Kooiker et al., 2005) was used to drive artificial microRNA (amiRNA) specifically suppressing *CWIN2* and *CWIN4* during ovule formation (amiRNA*CWIN24*). The *pSTK*::amiRNA*CWIN24* transgenic plants exhibited inhibition of ovule initiation and increased ovule abortion, which collectively resulted in >50% seed loss compared to the wild type. Surprisingly, measurement of the transcript levels of carbon (C) starvation reporter genes and manipulation of the source/sink ratio showed that the transgenic plants did not suffer from C starvation. This, together with the finding that assimilate is delivered symplasmically to the ovule primordia (Werner et al., 2011), shows that CWIN regulates ovule initiation through sugar signaling rather than provision of C nutrient. Further transcriptomic analyses support a model in which CWIN-generated hexose signals can be perceived by and transmitted through a cohort of plasma membrane HXTs or receptor-like kinases (RLKs) to modulate downstream candidate transcription factor (TF) and auxin signaling genes, thereby positively regulating ovule development.

RESULTS

CWIN2 and *CWIN4* Were Highly Expressed in the Floral Meristem, Ovule Primordia, and Young Ovules in Wild-Type Inflorescence

Among the four CWIN paralogs in Arabidopsis, *CWIN2* and *CWIN4* are known to be predominately expressed in reproductive organs (Schmid et al., 2005). As a first step to address the potential involvement of CWIN in ovule development, we performed in situ hybridization experiments to examine whether *CWIN2* and *CWIN4* were expressed in the cellular sites of ovule initiation.

The analysis revealed that *CWIN2* mRNA was detected in the inflorescence meristem and floral primordium (Fig. 1A), in comparison with the sense control (Fig. 1B). The signal intensity of the *CWIN2* transcript in the floral primordium appeared to increase from early stages 2 and 3 to late stage 5, when the primordia gave rise to gynoecium and stamens (Fig. 1A). The transcript was also evidently detected in gynoecium and stamens at stage 7 (Fig. 1A). Noticeably, strong expression of *CWIN2* mRNA was observed in the middle part of the gynoecium at stage 9 (Fig. 1C), where ovule initiation takes place (Smyth et al., 1990). The transcript was also detectable in the developing ovules at stage11 (Fig. 1D) and in anthers (Fig. 1, C and D, versus Fig. 1E). Interestingly, abundant expression of *CWIN2* was found in the stigma papillae at the top of the gynoecium at stage11 (Fig. 1D).

CWIN4 mRNA exhibited an expression pattern similar to that of *CWIN2* in the inflorescence meristem and floral primordia (Fig. 2). Evident expression of *CWIN4* was observed in the inflorescence meristem, floral primordium, and early floral organ primordia from stages 1 to 7 (Fig. 2, A and B), including primordia of gynoecium and stamen, in comparison with the sense control (Fig. 2C). Strong *CWIN4* mRNA signals were detected in the central part of the gynoecium when the ovule initiated at stage 9 (Fig. 2D), similar to the case for *CWIN2* (Fig. 1C). Expression of the *CWIN4* gene was also present in the developing ovules from stages 10 and 11 (Fig. 2, E and F) in comparison with the sense control (Fig. 2G). However, the *CWIN4* mRNA signal strength became weaker in the developing ovules

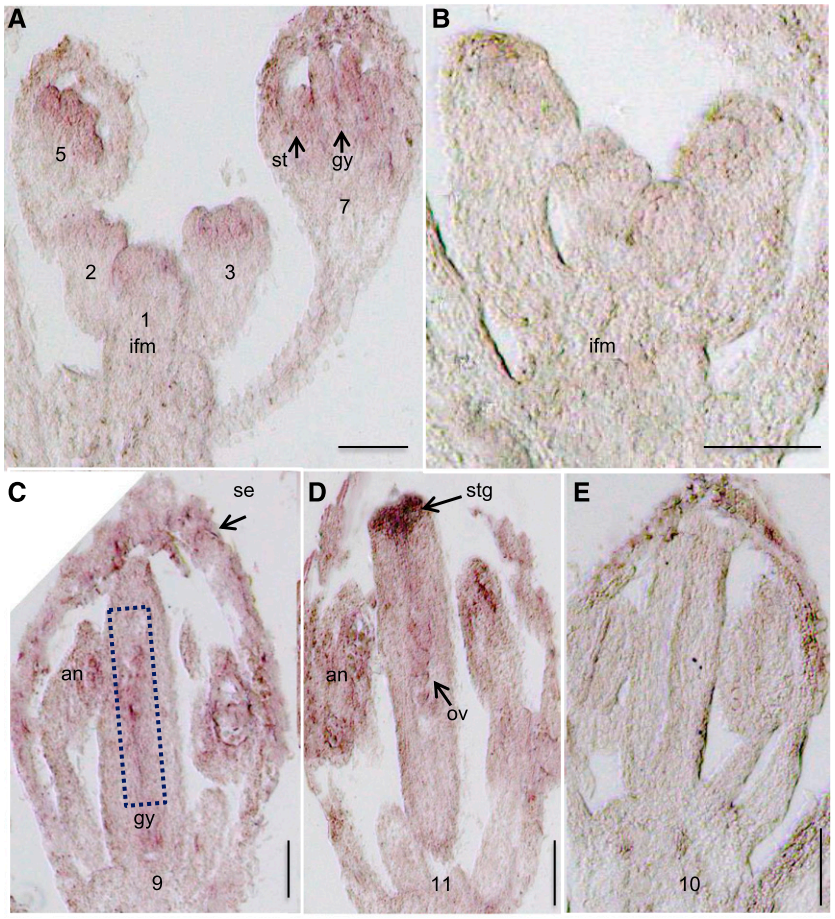

Figure 1. In situ hybridization for *CWIN2* mRNA on longitudinal inflorescence sections with the *CWIN2* antisense probe (A, C, and D) and sense probe (B and E) in wild-type (Col-0) Arabidopsis. A, *CWIN2* mRNA was detected in the inflorescence meristem (ifm) and floral primordia at stages 1 to 3. The transcript became abundant in floral primordia at stage 5, which gives rise to gynoecium (gy) and stamens (st) at stage 7. B, By contrast, no hybridization signal of CWIN2 was detected on the sections hybridized with a sense probe. C, By stage 9, *CWIN2* mRNA signal was observed in the middle part of the gynoecium, where ovules initiate (dashed rectangle). The transcript was also detected in anthers (an) and sepals (se). D, *CWIN2* mRNA was detected in the developing ovule (ov) at stage 11. Interestingly, a strong signal of *CWIN2* transcripts was detected in the stigma papillae (stg) tissue. E, Again, no hybridization signal was detected in the sense control. Scale bars = 200 μm. Numbers in the images indicate stages of floral development according to Smyth et al. (1990).

compared to that in the early stage of gynoecium (Fig. 2B) and ovule initiation (Fig. 2D).

pSTK::amiRNA*CWIN24* Transgenic Plants Displayed a Significant Reduction of *CWIN2* and *CWIN4* Transcript Levels at the Ovule Initiation Stage

The data from the in situ hybridization experiments indicate a possible role of *CWIN2* and *CWIN4* in ovule development. We thus further investigated whether disruption of *CWIN2* and *CWIN4* expression would affect ovule development. To achieve this, we employed an amiRNA approach to silence the expression of the two CWIN genes using an ovule-specific *pSTK* (Kooiker et al., 2005).

Through transgene screening and selection analyses, we obtained five independent transgenic lines homozygous for the transgene *pSTK*-amiRNA*CWIN24* at the T3 generation. Among them, lines 4-3, 80-4, and 106-2 displayed a severe reduction in seed number and silique length compared to those of the wild type (Supplemental Fig. S1). These lines were subsequently selected for detailed analysis. We first examined the expression level of *CWIN2* and *CWIN4* using a pooled sample of the flower buds from stages 8 to 10, when ovules initiate from the placenta (Figs. 1 and 2; Smyth et al., 1990). In comparison with the wild type, the transcript levels of *CWIN2* and *CWIN4* were reduced by 40% to 45% and 30% to 54%, respectively, in the transgenic lines (Fig. 3, A and B). We further investigated whether the reduction of *CWIN2* and *CWIN4* transcripts had any effect on the expression of other members of the INV family (*CWIN1*, *CWIN5*, *VIN1*, and *VIN2*; Wang and Ruan, 2012). None of these genes displayed altered expression levels compared to the wild type (Fig. 3, C–F). The findings indicate specific suppression of *CWIN2* and *CWIN4* in *pSTK*::amiRNA*CWIN24* transgenic plants.

We next examined whether suppression of *CWIN2* and *CWIN4* led to a decrease in CWIN activity. Here, enzyme activity was assayed on gynoecia-enriched samples that were carefully dissected from the same floral buds used for reverse transcription quantitative PCR (RT-qPCR) analysis. The dissection was based on the consideration that the ovule-specific STK-driven amiRNA*CWIN24* would specifically silence *CWIN2* and *CWIN4* in the placenta region and ovule primordia rather than in the surrounding tissues, such as anthers, sepals, and petals, where *CWIN2* and *CWIN4* were also expressed (Figs. 1 and 2). The enzyme assay revealed that CWIN activity was reduced by ~40% in transgenic lines 4-3 and 80-4 and by 18% in line 106-2 (Fig. 3G).

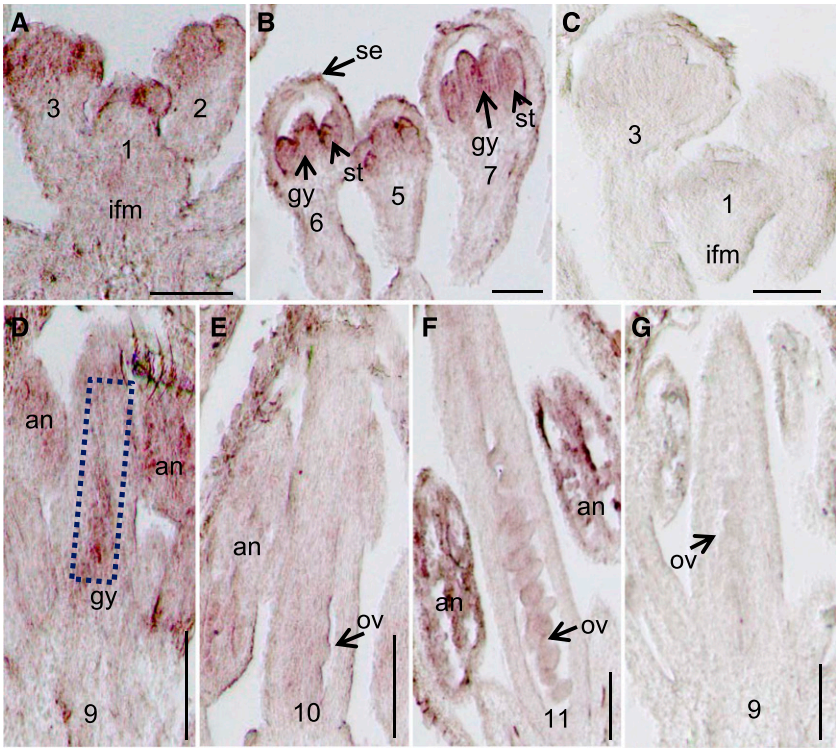

Figure 2. In situ hybridization for *CWIN4* on longitudinal inflorescence sections with the *CWIN4* antisense probe (A, B, and D–F) and sense probe (C and G) in wild-type Arabidopsis. A, *CWIN4* mRNA signal was detected in the inflorescence meristem (ifm) and through the early stages 2 and 3 of floral primordia. B, *CWIN4* transcript was abundant in floral primordia at stage 5, which gives rise to the formation of gynoecium (gy) and stamen (st). Here, at stage 6, *CWIN4* mRNA was evidently detected in early-stage gy and st, and this expression pattern remained at stage 7. No or little CWIN4 mRNA was detected in the sepal (se). C and G, Longitudinal sections of wild-type inflorescence hybridized with the *CWIN4* sense probe as a control. D, By stage 9, *CWIN4* mRNA was detected in the middle part of the gy, where ovules (ov) initiate (dashed rectangle). The transcripts were also detected in anthers (an) and sepals. E and F, *CWIN4* mRNA was detected in developing ov from stages 10 to 11. However, the signal was weaker than that at the early stages of gy and ov initiation (B and D). Noticeably, the transcript was highly expressed in the anther locule containing pollen grains (F). Scale bars = 200 μm. Numbers indicate stages of flower development according to Smyth et al. (1990).

Neither VIN nor CIN activities were affected in the transgenic lines (Fig. 3G).

Collectively, these data showed that the *pSTK*-driven amiRNA*CWIN24* specifically supressed *CWIN2* and *CWIN4* expression, leading to a reduction of CWIN activity at the ovule initatiation stage.

Silencing *CWIN* Inhibited Ovule Initiation and Induced Ovule Abortion

We then investigated whether silencing of *CWIN2* and *CWIN4* impacted ovule development. Phenotypic analyses revealed a significant reduction in silique length of the transgenic plants compared to that in the wild type (Fig. 4A) with average reduction of 50.8%, 62.6%, and 56% in seed number per silique in lines 4-3, 80-4, and 106-2, respectively (Supplemental Fig. S1; Supplemental Table S1).

To determine the developmental basis for the reduction in seed number, we counted the ovule number from cleared pistils dissected from flower buds at stages 10 to 11, prior to anthesis. The ovule number was significantly reduced in the transgenic lines to ~33 to 40 per pistil, as compared to ~59 in the wild type (Fig. 4, B and D; Supplemental Table S1). The pistil length was also reduced by 20% to 30% in the transgenic lines compared to that in the wild type (Fig. 4B).

The ratio of seed to ovule number was 0.95 in the wild type, but was reduced to ~0.62 to 0.74 in the transgenic lines (Supplemental Table S1), indicating aggravated ovule or seed abortion, manifested as gaps shown in the cleared siliques at stage 17 in the transgenic lines (Fig. 4A, red arrows). Under a dissection microscope, a substantial number of residual white structures were clearly observed in the transgenic siliques (Fig. 4C, red asterisks), a phenotype hardly observed in the wild-type siliques. The tiny white dots in the transgenic lines morphologically resembled ovule abortion (Ebel et al., 2004). However, we cannot rule out the possibility that some may be residuals derived from early seed abortion. On average, there were 10, 12, and 15 tiny white dots (designated as ovule or seed abortion) per silique in lines 4-3, 80-4, and 106-2, respectively, as compared to only three in the wild-type siliques, hence constituting a higher abortion rate in the transgenic lines (Fig. 4E).

Based on the knowledge of ovule number per pistil (Fig. 4B; Supplemental Table S1), the number of ovules blocked from initiation in the transgenic pistils was calculated by subtraction of the number of transgenic ovules from that of wild-type ovules. It was found that on average 22, 26, and 20 ovules were blocked from initiation in lines 4-3, 80-4, and 106-2, respectively (Supplemental Table S1), accounting for ~60% to 70% of seed loss, with the remaining ~30% to 40% loss derived from ovule or seed abortion (Fig. 4, D and F). These findings demonstrate that blockage of ovule initiation is the primary cause of reduction in seed number, with ovule or seed abortion contributing to additional seed loss in the transgenic plants.

Blockage of Ovule Initiation Was Not Caused by C Starvation in the CWIN-Silenced Plants

In Arabidopsis, Suc supply to young ovules follows a symplasmic pathway, as evidenced by the unloading of GFP and fluorescent tracers from the placenta SE/CC to the ovule primordia at floral stage 9 (Werner et al., 2011). Given that CWIN typically plays a role in

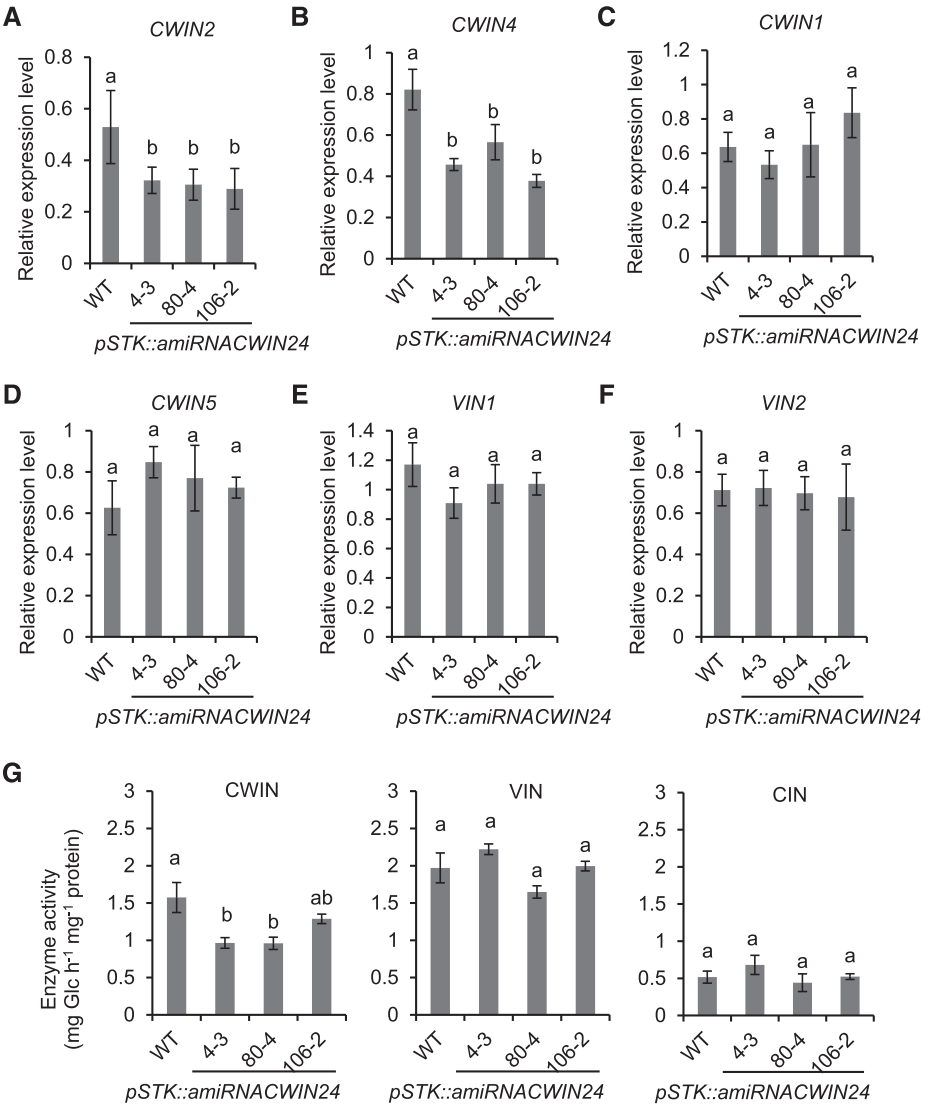

Figure 3. Specific silencing of *CWIN2* (A) and *CWIN4* (B) without impacting other CWIN paralogous genes (C and D) and *VINs* (E and F) in *pSTK*::amiRCWIN24 transgenic lines. RT-qPCR analysis was conducted using a pool of flower buds from stages 8 to 10, when the ovule initiates from placenta (Smyth et al., 1990). Each value is the mean ± SE of at least four biological replicates for each independent transgenic line. One replicate was from a pooled sample comprised of ~10 flower buds at stages 8 to 10 harvested from one plant. Different lowercase letters over bars indicate significant difference ($P \leq 0.05$, one-way ANOVA). G, Reduction of CWIN activity in the *pSTK*::amiRNACWIN24 transgenic plants compared to the wild type. Note that there is no difference in VIN and CIN activity between wild-type and transgenic plants. Each value is the mean ± SE of five biological replicates. Each replicate was comprised of pooled gynoecium samples that were dissected from flower buds at stages 8 to 10 from more than three individual plants. Different lowercase letters over bars indicate significant difference ($P \leq 0.05$, one-way ANOVA).

apoplasmic phloem unloading and postphloem transport (e.g. Jin et al., 2009, Palmer et al., 2015), it is intriguing from a C nutrient perspective that silencing of *CWIN2* and *CWIN4* inhibited ovule initiation (Figs. 3 and 4). We thus conducted experiments to examine whether inhibition of ovule initiation in the CWIN-suppressed transgenic plants was due to insufficient C availability.

We reasoned that if the blockage of ovule initiation in the transgenic plants (Fig. 4) was due to shortage of assimilate supply, the ovule inhibition phenotype could be rescued or alleviated by supplying the ovules with more C nutrient. To test this, we trimmed two-thirds of the developing siliques to increase the source-to-sink ratio (Fig. 5A), thereby allowing more assimilates to be available to form new ovules and siliques. As shown in Figure 5, B to E, increasing the C availability to the shoot apical floral meristem failed to recover any of the phenotypes in silique length and ovule or seed number of the transgenic plants compared to those of untreated transgenic plants, except in line 4-3, where trimming increased the silique length slightly.

To directly investigate whether the transgenic floral buds were under C starvation, we measured the transcript levels of three C starvation report genes, *ATL8* (*At1g76410*), *KMD4* (*At3g59940*), and *OLEOSIN7* (*At5g56100*), that are strongly induced in the flower buds at stages 8 to 10 under sugar-depletion conditions (Lauxmann et al., 2016). RT-qPCR analysis revealed that none of these genes was induced in the transgenic plants (Fig. 6). The above findings indicate that *pSTK*-amiRNA*CWIN24* plants did not suffer from C starvation and the ovule phenotype did not arise from insufficient C supply.

RNA-Sequencing Analysis between *pSTK*-amiRNA*CWIN24* and Wild-Type Plants: Overall Quality and Reliability Assessment

To explore the underlying basis of CWIN-mediated ovule initiation, RNA-sequencing (RNA-seq) was conducted to compare the transcript profiles of flower buds

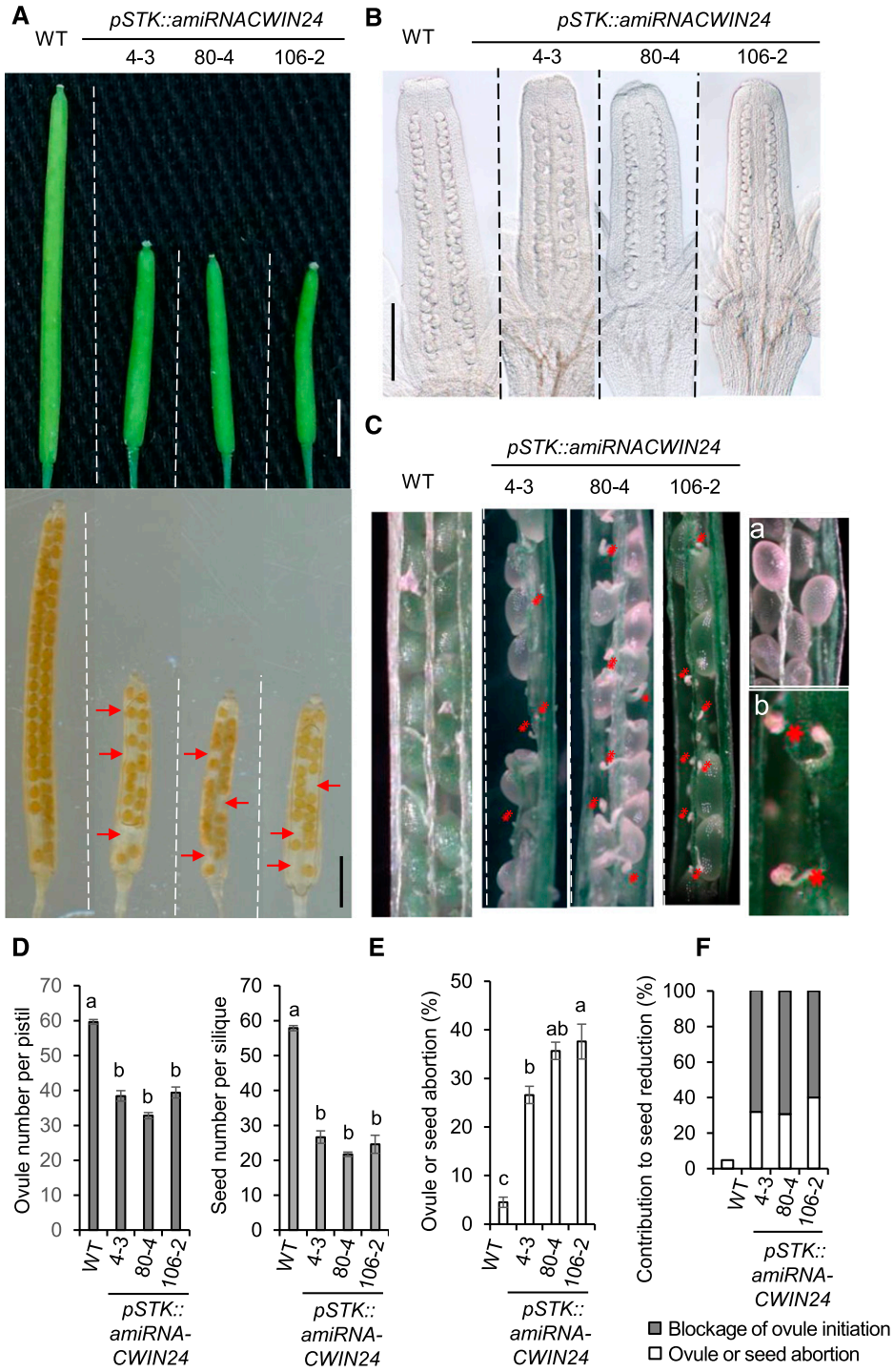

Figure 4. pSTK::amiRNACWIN24 transgenic plants exhibited blockage of ovule initiation and aggravated ovule or seed abortion. A, Representative images of fully expanded siliques (top) and their corresponding cleared siliques (bottom) of the wild type (WT) and three independent transgenic lines harvested at flower stage 17. Red arrows point to vacancies inside the siliques, indicating aborted ovules or seeds. Scale bars = 2 mm. B, Representative differential interference contrast images of ovules in pistils of the wild type and three transgenic lines at flower stages 10 to 11, prior to anthesis. Note the reduced pistil length and ovule number in the transgenic lines compared to the wild type. Scale bar = 100 μm. C, A substantial portion of ovules/seeds was aborted in transgenic siliques, as compared to the wild type, at stage 17. Asterisks indicate aborted ovules or seeds. Insets a and b are magnified views of normal seed and aborted ovules/seeds, respectively. D, Ovule number per pistil and seed number per silique. Each value is the mean ± SE, with data collected from at least three biological replicates for each line. Different lowercase letters over bars indicate significant difference relative to the wild type ($P < 0.05$, one-way ANOVA). E, The percentage of aborted ovules or seeds per silique was calculated by dividing the number of total ovules by the number of aborted seed or ovules documented in Supplemental Table S1. Each value is the mean ± SE, with data collected from at least five biological replicates for each line. Different lowercase letters over bars indicate significant differences ($P < 0.05$, one-way ANOVA). F, Contribution of blockage of ovule initiation and ovule or seed abortion to seed number reduction.

pooled from stages 8 to 10 in a representative transgenic line, 4-3, and the wild type. After trimming, an average of 58.11 million and 55.58 million clean reads were obtained from four biological replicates of the wild-type and transgenic plants, respectively. Approximately 90% of the clean reads were uniquely mapped to The Arabidopsis Information Resource genome reference (TAIR10; Supplemental Fig. S2A). Principal component analysis (PCA) of the transcriptome revealed a clear separation between the transgenic line and the wild type and showed that the biological replicates were clustered closely in each genotype, with no outlier detected (Fig. 7A). Hence, all replicates from each genotype were used for subsequent identification of differentially expressed genes (DEGs). A total of 1,940 DEGs were identified between transgenic and wild-type plants (Supplemental Table S2), of which 408 were upregulated and 1,082 were downregulated (Fig. 7B).

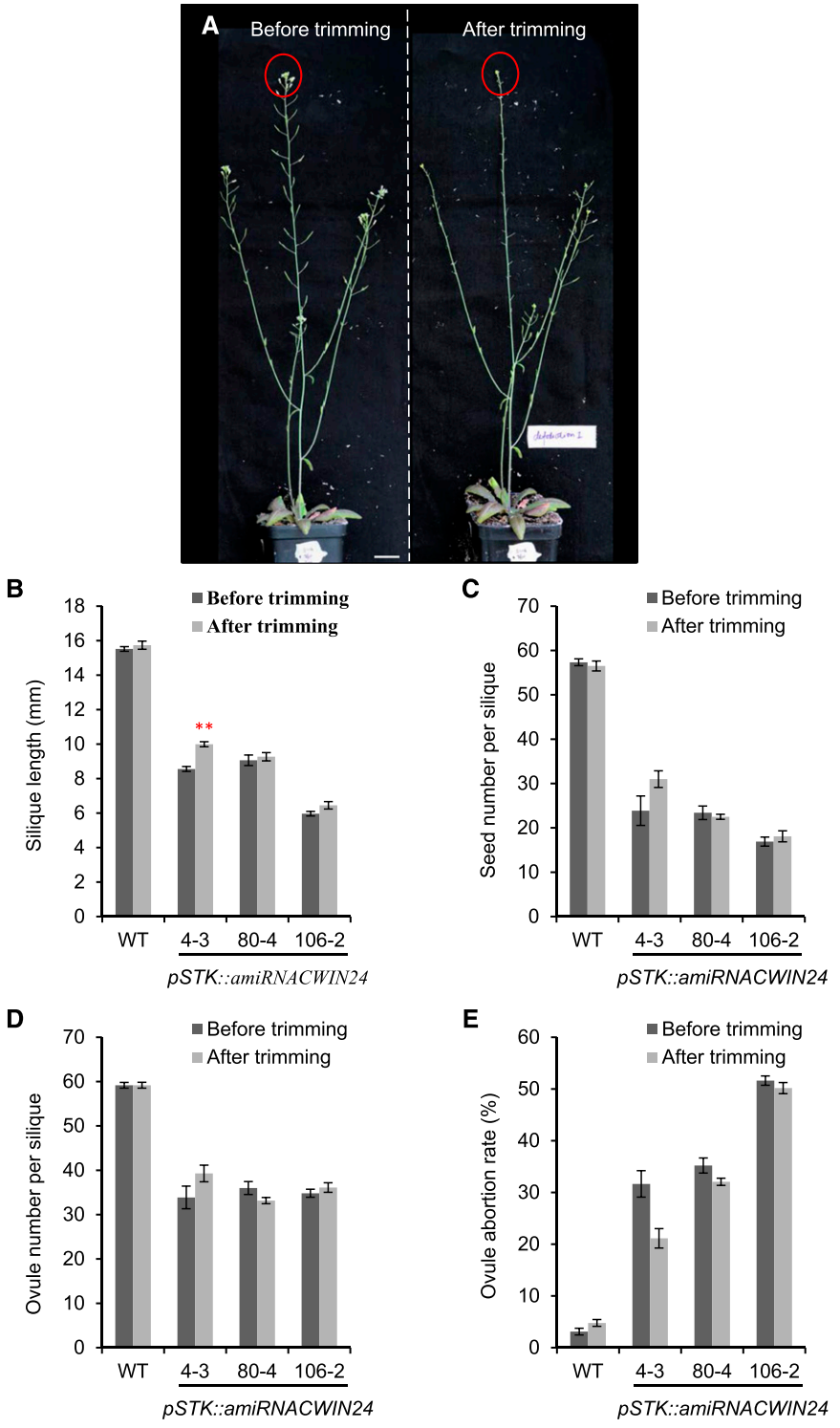

Figure 5. Increasing C nutrient availability to the newly formed floral buds by trimming two-thirds of the developed siliques did not recover the ovule phenotype in the *pSTK*::amiRNACWIN24 transgenic plants. A, Thirty-five-day-old Arabidopsis plant before (left) and after (right) trimming. The newly developed siliques from the shoot apex (red circles) were counted and measured at ~5 d after anthesis, at flower stage 17, when the siliques were fully expanded. Scale bar = 0.4 cm. B to E, Statistical analysis of silique length (B), seed number per silique (C), ovule number per silique (D), and percentage of aborted ovule of total ovule per silique (E) before and after trimming in pSTK::amiRNACWIN24 transgenic plants. Each value is the mean ± SE, with data collected from at least six biological replicates; each replicate was comprised of counts from 5 to 10 fully expanded siliques harvested from one individual plant. The double asterisk indicates significant difference relative to the wild type (WT; $^{**}P \leq 0.01$, Student's *t* test).

To validate the RNA-seq analysis, we selected a subset of genes for RT-qPCR analysis across the *pSTK*-amiRNA*CWIN24* transgenic line and the wild type using the same samples as for RNA-seq. The analysis revealed that the transcript fold change (FC) of the seven selected genes from RT-qPCR measurement was consistent overall with that of RNA-seq (Supplemental Fig. S2B). It was noted that the FC measured by RT-qPCR was generally lower than that from the RNA-seq analysis, probably due to RNA-seq being more sensitive and specific than RT-qPCR (Griffith et al., 2010). Importantly, correlation analysis of these two data sets revealed a R^2 value of 0.6756 (Supplemental Fig. S2C), which is within the range of reported

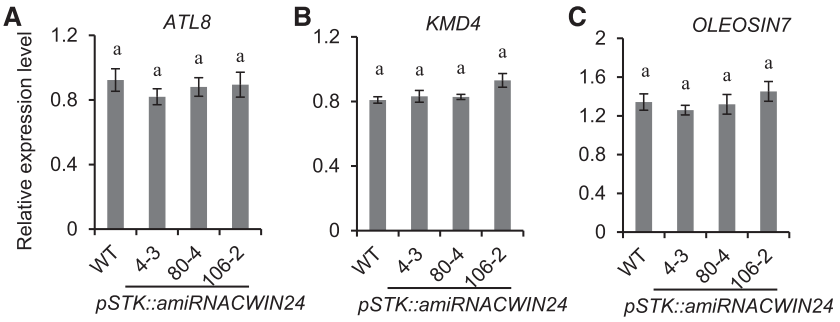

Figure 6. Expression of three C-starvation reporter genes (A–C) was not affected in the *pSTK*::amiRNACWIN24 transgenic plants in flower buds at stages 8 to 10, when ovules initiate from placenta. Each value is the mean ± SE, with data collected from at least five biological replicates (five individual plants) for each independent transgenic line. Lowercase letters over bars indicate significant difference ($P \leq 0.05$, one-way ANOVA). WT, Wild type.

correlations between RNA-seq and RT-qPCR results (Xu et al., 2011). Together, the analyses indicate the reliability of our RNA-seq data.

A Large Number of Early Auxin-Responsive Genes Were Downregulated in Response to CWIN Silencing

Given the increasing number of studies indicating that sugar-hormone interaction plays a role in modulating plant development (León and Sheen, 2003; Wang and Ruan, 2013) and the importance of hormones in ovule initiation (Cucinotta et al., 2014), we closely examined hormone-related DEGs from the transgenic and wild-type plants.

In total, 49 DEGs were classified in the hormone category, which was subclassed into six groups (Fig. 7C). Among them, genes involved in auxin, abscisic acid, and ethylene metabolism were the top three groups, representing 53%, 16%, and 14% of the total hormone genes, respectively. Genes involved in gibberellin (GA), jasmonate (JA), and cytokinin (CK) pathways were each <10% of the total hormone-related genes (Fig. 7C). These findings indicate that in comparison with other hormone pathways, auxin-related genes appear to be affected the most in response to CWIN suppression.

Among the 26 auxin-related genes, the majority (19 of 26) were early auxin response genes (Table 1). Remarkably, these early auxin response genes were all downregulated in response to CWIN suppression, which includes 14 *SMALL AUXIN UP RNAs* (*SAURs*), four *AUX/IAA*s, and one *GH3*. *AUX/IAA* encodes a short-lived nuclear protein that functions as a repressor against auxin-inducible gene expression, in which AUX/indole-3-acetic acid (IAA) forms a heterodimer with auxin response factors (ARFs) to repress the transcriptional activity of ARF genes (Hayashi, 2012). *GH3* encodes an enzyme that catalyzes the conjugation of IAA with amino acids to yield an inactive storage form of IAA (Ludwig-Müller, 2011), thereby modulating the intracellular IAA level. Among the 14 *SAURs* downregulated in the CWIN-silenced samples, eight, *SAUR1*, *SAUR4*, *SAUR12*, *SAUR21*, *SAUR29*, *SAUR64*, *SAUR67*, and *SAUR70*, were auxin inducible, and one, *SAUR6*, was auxin repressive (Ren and Gray, 2015); functions for the remaining five *SAURs* remain unknown.

A Cohort of MADS-Box TFs Were Downregulated in *pSTK*-amiRNA*CWIN24* Plants, and Overexpression of One of Them, *STK*, Partially Complemented the Silique and Seed Phenotype

A total of 76 DEGs encoding TFs (classified into 30 TF families) were identified from the transgenic samples (Supplemental Table S3), representing 5.1% of the 1,490 DEGs. This was done by searching the Arabidopsis transcription database (PlantTFDB), which contains 2,996 TFs classified into 58 families (Jin et al., 2017). Previous studies in Arabidopsis have found that most of the TFs that function in ovule formation belong to the MADS-box family, including *SHATTERPROOF1* (*SHP1*), *SHP2*, and *STK*, which form a monophyletic clade with *AGAMOUS* (*AG*), sharing a common function in determining ovule identity and exhibiting overlapping expression patterns in ovule primordia (Pinyopich et al., 2003; Skinner et al., 2004). Indeed, RNA-seq analysis revealed that members of two subfamilies of the MADS family were significantly downregulated in response to *CWIN* suppression, including three MICK_MADS TFs, *STK* (formerly *AGL11*), *AGL66*, and *AGL104*, and one M_type_MADS TF, *AGL94* (Table 2). These findings suggest that MADS TFs may function as downstream targets of CWIN-mediated ovule initiation pathways. Interestingly, among the three ovule identity genes, *SHP1*, *SHP2*, and *STK*, only *STK* was downregulated in response to CWIN silencing, suggesting that CWIN-mediated ovule initiation may be exerted, in part, through modulation of *STK* expression.

To test this possibility, *STK*, driven by its native promoter, was overexpressed in the transgenic background to test whether overexpression could complement the ovule phenotype. Here, a *pSTK*::STK (coding sequence [CDS]) overexpression construct was transformed into transgenic line 4-3. Two homozygous complementation lines, 2-9 and 7-7, were identified that exhibited partial recovery of the silique-length phenotype compared to the wild type and CWIN-silencing

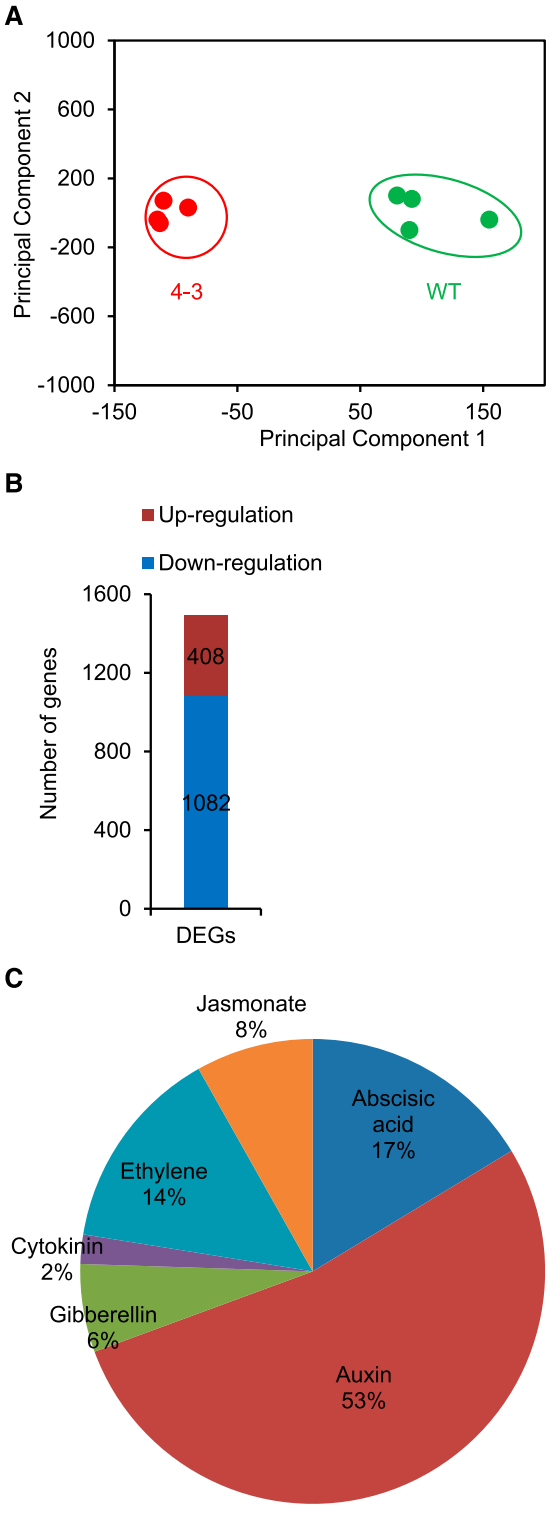

Figure 7. RNA-seq analyses of DEGs during ovule initiation in *pSTK*-amiRNACWIN24 transgenic line 4-3 as compared to the wild type. A, PCA of transcripts between transgenic and wild-type plants during ovule initiation. B, Number of genes differentially expressed during ovule initiation in the CWIN-silenced transgenic plants compared to the wild type. C, Percentage of each class of hormone-related DEGs in the transgenic plants during ovule initiation. The number of DEGs in each class was expressed as a percentage of the total 49 hormone-related DEGs. Four biological replicates were used for each genotype in this RNA-seq analysis, with each replicate comprised of 10 to 15 buds from one plant.

line 4-3 (Fig. 8A). The *STK* mRNA level was fully recovered and increased in complementation lines 7-7 and 2-9, respectively (Fig. 8B), leading to partial complementation of the silique-length and seed-number phenotypes (Fig. 8, C and D), due to partial recovery of ovule number and alleviated abortion in lines 2-9 and 7-7 (Fig. 8, E and F).

pSTK-amiRNA-Mediated Silencing of *CWIN* Altered the Expression of Genes Encoding RLKs and Small GTPases

As described above, a wide variety of hormone-related and TF genes exhibited differential expression in response to CWIN suppression. This, together with the findings that CWIN may regulate ovule initiation through sugar signaling (Figs. 5 and 6), suggests that alteration in sugar concentration or flux by modulating CWIN in the extracellular region must be sensed, probably by plasma membrane proteins (Ruan, 2014), for transduction of the signal into the intracellular space to regulate gene expression. Consistent with this view, 23 of 28 DEGs encoding RLKs, showed increased expression during ovule initiation in response to CWIN silencing (Table 3). RLKs are a group of transmembrane proteins with an N-terminal extracellular domain, a transmembrane span, and a cytosolic protein kinase domain that are involved in a wide range of signal perception and transduction activities (Wu et al., 2016). We also found 15 DEGs encoding small GTPase-related proteins; all of them exhibited decreased expression during ovule initiation in the CWIN-suppressed plants compared to wild-type plants (Table 3). Apart from the small GTPase genes, three genes encoding regulatory proteins of Rho GTPase were also observed (Table 3). These include Rho of plants (Rop) guanine nucleotide exchange factor 9 (ROPGEF9) and two Rho GTPase effector proteins, RIC1 and RIC3 (Vernoud et al., 2003)

We also noticed that two wall-associated kinase (WAK) genes, *WAK1* and *WAK2*, were upregulated in response to CWIN silencing (Table 3). WAKs represent a unique class of RLKs that contain an extracellular domain that physically links with the pectin molecules of the cell wall and a cytoplasmic Ser/Thr kinase domain (Kohorn et al., 2006).

Hexose Transporter Genes Were Largely Repressed in Response to CWIN Silencing during Ovule Initiation

Suc hydrolysis by CWIN generates Glc and Fru in the extracellular space, which are then taken up across the plasma membrane by HXTs into the adjacent cells, with

Table 1. *A large number of auxin signaling-related genes were downregulated during ovule initiation in* pSTK-*amiRNA*CWIN24 *transgenic plants compared with the wild type*

RPKM values were derived from four biological replicates of floral buds at stages 8 to 10, when ovules initiate, with each replicate comprised of 10 to 15 buds from one plant.

Name	Average RPKM		Log_2 FC	Annotation
	Wild Type	Transgenic		
IAA5	4.85	1.24	−2.22	IAA5 (IAA Inducible 5)
IAA19	15.25	7.62	−1.11	IAA19 (IAA Inducible 19)
IAA14	1.25	0.51	−1.31	IAA14 (IAA Inducible 14)
IAA1	20.22	9.24	−1.22	IAA1(IAA Inducible 1)
SAUR64	1.40	0.64	−1.19	Auxin-responsive protein, putative; auxin inducible
SAUR67	5.71	2.90	−1.03	SAUR67; auxin inducible
SAUR6	7.64	3.79	−1.09	Auxin-responsive protein, putative; auxin repressive
SAUR12	10.83	5.57	−1.08	Auxin-responsive protein, putative; auxin inducible
SAUR29	1.16	0.48	−1.79	Auxin-responsive protein, putative; auxin inducible
SAUR47	1.37	0.08	−4.42	Auxin-responsive protein, putative
SAUR39	3.55	0.21	−4.2	Auxin-responsive protein-related
SAUR49	19.61	8.61	−1.28	Auxin-responsive protein, putative
SAUR1	2.10	1.00	−1.18	Auxin-responsive family protein; auxin inducible
SAUR3	2.55	0.87	−1.7	Auxin-responsive family protein
SAUR4	2.93	1.40	−1.13	Auxin-responsive family protein; auxin inducible
SAUR5	2.83	0.95	−1.64	Auxin-responsive family protein
SAUR21	4.63	2.33	−1.06	Auxin-responsive protein, putative; auxin inducible
SAUR70	8.38	3.81	−1.21	Auxin-responsive protein, putative; auxin inducible
AT5G13350	3.99	0.58	−2.88	Auxin-responsive GH3 family protein
YUC4	0.54	1.18	1.06	Auxin biosynthesis
YUC2	5.04	2.39	−1.15	Auxin biosynthesis
AT1G54070	1.30	0.06	−4.6	Dormancy/auxin associated protein-related
DRMH2	71.75	4.59	−4.05	Dormancy/auxin associated family protein
AT5G47530	8.02	1.32	−2.66	Auxin-responsive protein, putative
BIG	4.10	9.16	1.06	BIG, a positive regulator of polar auxin transport
AT2G04852	0.79	1.97	1.22	Locus overlaps with AT2G04850

coregulation between the two observed in many cases (Ruan, 2014; Li et al., 2017; Wang et al., 2019). We therefore examined how sugar transporter genes may have responded to silencing of CWINs in the *pSTK*-amiRNACWIN24 plants.

We identified 9 DEGs encoding HXTs, including *SWEET*s, *Sugar Transporter*s (*STP*s), and a tonoplast monosaccharide transporter (*TMT*). They were all downregulated in the CWIN-silenced transgenic plants (Table 3). Among these nine DEGs, five encode clade I or II *SWEET* HXTs (Eom et al., 2015), including *SWEET3*, *SWEET4*, *SWEET5*, *SWEET7*, and *SWEET8*, and three encode *STP*s, including *STP2*, *STP6*, and *STP9*. A functional assay in yeast cells revealed that STP9 mediated specific uptake of Glc in a proton-dependent manner (Büttner, 2010). STP2 and STP6 were characterized as high-affinity transporters of monosaccharides including Glc, Man, and the pentose Xyl, with STP6 carrying additional capacity to transport Fru (Büttner, 2010). Apart from the above eight HXTs predicted to operate on plasma membranes, *TMT3* was also downregulated. Interestingly, expression of two Arabidopsis H^+-ATPase (*AHA*) genes, *AHA6* and *AHA9*, was also downregulated in the *pSTK*-amiRNA*CWIN24* transgenic line compared to the wild type (Table 3). AHA functions to promote proton pumping to the apoplast (Hager, 2003), which generates the driving force for sugar uptake mediated by proton-coupled sugar symporters.

Table 2. *Genes encoding several MADS TFs were downregulated in* pSTK-*amiRNA*CWIN24 *transgenic plants compared with the wild type during ovule initiation*

RPKM values were derived from four biological replicates of floral buds at stages 8 to 10, when ovules initiate, with each replicate comprised of 10 to 15 buds from one plant.

TF Family	Gene Identifier	Gene Name	Average RPKM		Log_2 FC
			Wild Type	Transgenic	
MIKC_MADS	AT4G09960	STK	9.82	0.60	−4.37
	AT1G77980	AGL66	2.65	0.60	−2.26
	AT1G22130	AGL104	6.95	1.65	−2.17
M-type_MADS	AT1G69540	AGL94	5.05	1.68	−1.71

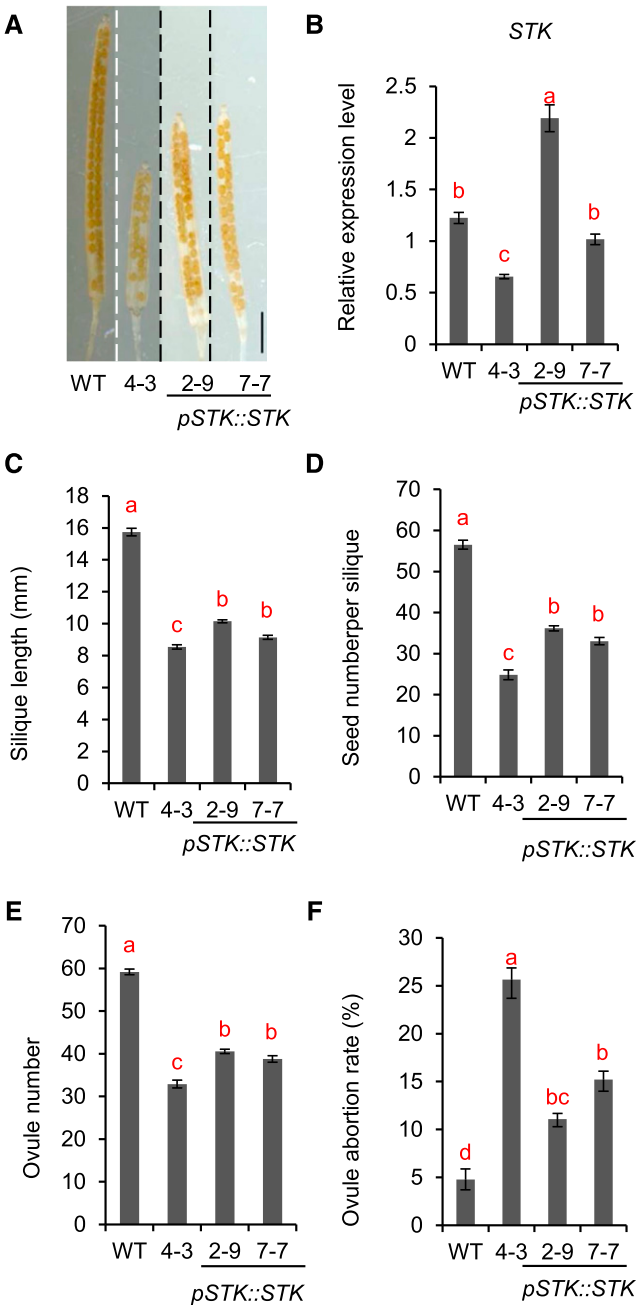

Figure 8. Expression of *pSTK*::STK (CDS) in pSTK-amiRNACWIN24 (line 4-3) background partially recovered the phenotype of ovule defects. A, Representative images of cleared siliques of the wild type (WT), *pSTK*-amiRNACWIN24 transgenic line (4-3), and two independent homozygous complementation lines, 2-9 and 7-7, expressing *pSTK*::STK in *pSTK*-amiRNACWIN24 (4-3) transgenic background at the fully expanded stage, flower stage 17. Scale bar = 2 mm. B, RT-qPCR analysis revealed that the expression *STK* was fully restored in complementation line 7-7, with expression exceeding the wild-type level in line 2-9. Samples were harvested from a pool of flower buds at stages 8 to 10, when ovule initiates from placenta (Smyth et al., 1990). C to F, Statistical analyses of silique length (mm; C), seed number per silique (D), ovule number per silique (E), and percentage of aborted ovule of total ovule per silique (F). Each value is the mean ± SE of at least five biological replicates (five individual plants) for each independent transgenic line. Different lowercase letters over bars indicate significant difference ($P \leq 0.05$, one-way ANOVA).

By contrast, none of the DEGs found for Suc transporters was expressed in the CWIN-silenced plants.

The downregulation of nine HXT genes in response to CWIN silencing prompted us to further examine whether they are spatially coexpressed with *CWIN2* and *CWIN4* during ovule initiation. To achieve this, we performed in situ hybridization on sections of floral buds from stages 8 to 10 in wild-type plants. We selected *SWEET8* and *STP9* as representatives of the respective *SWEET* and *STP* subfamilies, because they displayed high transcript levels during ovule initiation in the wild type (Table 3). In comparison with the sense probe control (Fig. 9A), the *STP9* mRNA signal was detected in sections of floral buds at stages 8 to 10 (Fig. 9, B–D). Its transcript signals were observed in the middle part of the gynoecium before ovule primordia initiation at stage 8, in the initiating ovule primordia at stage 9, and in developing ovules at stage 10 (Fig. 9, B–D). A similar expression pattern was observed for *SWEET8* mRNA (Fig. 9, E–H). Overall, the expression patterns of *STP9* and *SWEET8* overlapped with that of *CWIN2* and *CWIN4* (Figs. 1 and 2).

DISCUSSION

CWIN Plays an Essential Role in Ovule Initiation through Sugar Signaling Rather Than Provision of Carbon Nutrients

CWIN-mediated Suc metabolism and signaling is central to plant development, including the formation of pollen fertility, seed and fruit set, and stress response (Ruan et al., 2010; Ruan, 2014). It remains unknown, though, whether and how CWIN plays a role in ovule formation, a prerequisite for seed production. Here, we provide molecular and developmental evidence that CWIN plays a critical role in ovule initiation and growth in Arabidopsis. Among the *CWIN* gene family in Arabidopsis, *CWIN2* and *CWIN4* are predominately expressed in reproductive organs (Schmid et al., 2005), in which the two CWINs may play complementary or additive roles. In situ hybridization experiments revealed high expression of *CWIN2* and *CWIN4* mRNAs in the placenta region, where ovules initiate (Figs. 1 and 2). Ovule-specific silencing of *CWIN2* and *CWIN4* using the amiRNA approach resulted in significant and specific reduction of *CWIN2* and *CWIN4* transcripts, leading to a decrease in CWIN activity without impacting *VIN* and *CIN* expression or activity (Fig. 3). This molecular intervention reduced the seed number by >50% compared to that in the wild type, mainly due to blockage of ovule initiation and, to a less extent, aggravated ovule abortion (Fig. 4). These findings demonstrate that CWIN is critical for ovule initiation and differentiation. The findings fill a major

Table 3. *Genes encoding RLKs, small GTPases, and HXTs were differentially expressed in* pSTK-*amiRNA*CWIN24 *during ovule initiation compared with the wild type*

RPKM values were derived from four biological replicates of floral buds at stages 8 to 10, when ovules initiate, with each replicate comprised of 10 to 15 buds from one plant.

Functional Category	Gene Identifier	Average RPKM		Log_2 FC	Annotation
		Wild Type	Transgenic		
Signaling					
RLKs	AT5G59670	4.06	8.89	1.05	LRR protein kinase, putative
	AT2G07040	1.79	0.08	−4.51	ATPRK2A, PRK2A | PRK2A;
	AT5G07620	1.25	4.26	2	Protein kinase family protein
	AT4G20790	1.25	0.52	−1.36	LRR family protein
	AT1G07650	11.63	27.88	1.17	LRR transmembrane protein kinase
	AT1G53430	6.6	15.24	1.1	LRR family protein/protein kinase family protein
	AT1G56120	0.63	1.39	1.02	Receptor kinases LRR VIII.VIII-2
	AT1G34420	0.68	1.47	1.31	LRR family protein/protein kinase family protein
	AT1G09970	20.98	52.69	1.24	LRR XI-23 | LRR XI-23
	AT4G28490	2.84	6.41	1.08	RLK5 HAE (HAESA)
	AT5G25930	1	3.04	1.52	LRR family protein/protein kinase family protein
	AT1G35710	3.38	7.4	1.36	LRR transmembrane protein kinase, putative
	AT3G47570	0.81	1.75	1.02	LRR transmembrane protein kinase, putative
	AT4G08850	8.47	18.22	1.19	Receptor kinases LRR XII
	AT4G39270	4.35	6.57	1	LRR transmembrane protein kinase, putative
	AT2G23200	4.48	10.12	1.28	Protein kinase family protein
	AT5G54380	11.16	23.85	1.02	THE1 (THESEUS1); protein kinase
	AT4G21410	3.73	8.33	1.05	Protein kinase family protein
	AT4G23130	1.11	2.56	1.12	CRK5 (Cys-rich RLK5)
	AT4G23140	0.76	2.07	1.34	CRK6 (Cys-rich RLK6)
	AT4G23230	0.8	2.26	1.4	Protein kinase family protein
	AT1G66880	3.39	7.47	1.15	Ser/Thr protein kinase family protein
	AT5G38240	1	2.96	1.45	Ser/Thr protein kinase, putative
	AT2G18470	3.56	0.48	−3.02	Protein kinase family protein
	AT4G34440	1.32	0.49	−1.54	Protein kinase family protein
	AT3G12000	9.18	4.25	−1.18	S-locus-related protein SLR1, putative (S1)
	AT1G21250	7.22	21.76	1.49	WAK1 (Cell wall-associated kinase 1)
	AT1G21270	2.41	5.28	1.03	WAK2 (Cell wall-associated kinase 2)
Small GTPases	RIC1	1.48	0.23	−2.61	Rop-Interactive Crib motif-containing protein 1
	RIC3	4.92	0.54	−3.3	Rop-Interactive Crib motif-containing protein 3
	ROP1	7.91	3.02	−1.48	Rho-related protein from plants 1; GTP binding
	ROP7	3.89	1.48	−1.44	Arabidopsis RAC-like 2; GTP binding
	AT1G08340	8.18	2.9	−1.58	Rac GTPase activating protein, putative
	RABA2B	9.76	4.7	−1.13	Arabidopsis rab GTPase homolog a2b
	RABA4D	2.69	0.74	−1.99	RAB GTPase homolog A4d, GTP binding
	RABH1e	7.55	2.85	−1.47	Arabidopsis Rab GTPase homolog H1e, GTP binding
	RABA6a	4.8	2.38	−1.11	Arabidopsis Rab GTPase homolog A6a, GTP binding
	ROPGEF9	1.1	0.36	−1.66	ROPGEF9, Rho guanyl-nucleotide exchange factor
	PRA1.B5	2.85	1.32	−1.57	PRA1.B5 (Prenylated Rab Acceptor 1.b5)
	AT2G37290	1.84	0.94	−1.05	Rab GAP/TBC domain-containing protein
	AT5G09550	36.17	7.65	−2.33	RAB GDP-dissociation inhibitor
	AT1G12070	3.04	0.34	−3.28	Rho GDP-dissociation inhibitor family protein
	AT1G62450	10.99	1.72	−2.78	Rho GDP-dissociation inhibitor family protein
Sugar Transporters and Water Channel					
Sugar transporters	SWEET3	33.58	17.98	−0.98	HXT
	SWEET4	15.96	9.34	−0.88	HXT
	SWEET5	9.96	0.99	−3.41	HXT
	SWEET7	26.03	10.71	−1.38	HXT
	SWEET8	132.86	57.57	−1.3	HXT
	STP2	76.32	33.43	−1.28	STP2, Glc:hydrogen symporter
	STP6	17.54	1.79	−3.35	STP6, Glc:hydrogen symporter
	STP9	68.39	7.04	−3.4	STP9, Glc:hydrogen symporter
	TMT3	10.95	2.87	−2.14	TMT3 (tonoplast monosaccharide transporter3)
	TIP1-3	18.01	2.2	−3.13	TIP1;3 (tonoplast intrinsic protein 1;3)

(*Table continues on following page.*)

Table 3. (*Continued from previous page.*)

Functional Category	Gene Identifier	Average RPKM		Log_2 FC	Annotation
		Wild Type	Transgenic		
	TIP5-1	10.88	2.64	−2.13	TIP1;5 (tonoplast intrinsic protein 1;5)
	PIP1-5	77.28	39.66	−1.06	PIP1;5 (plasma membrane intrinsic protein 1;5)
	PIP2-4	26.34	12.76	−1.14	PIP2;4 (plasma membrane intrinsic protein 2;4)
	PIP2B	31.94	14.62	−1.21	PIP2B (plasma membrane intrinsic protein 2b)
	PIP2-3	31.16	13.01	−1.36	PIP2;3 (plasma membrane intrinsic protein 2;3)
H^+-ATPases	AHA6	49.51	9.1	−2.53	AHA6 (Arabidopsis H+-ATPase 6)
	AHA9	36.46	8.08	−2.28	AHA9 (Arabidopsis H+-ATPase 9)

knowledge gap in our understanding of roles of sugar metabolism or signaling in reproductive development and offer opportunities to potentially improve ovule development and hence seed yield.

CWIN could contribute to sink development by facilitating phloem unloading of Suc and converting it to Glc and Fru as major nutrients and energy sources. It is thus possible that the blockage of ovule formation in the CWIN-silenced plants may be due to starvation of C nutrient in the floral buds. However, this is highly unlikely based on the following analyses.

First, artificially increasing assimilate availability to the newly forming floral buds of transgenic plants by increasing source-to-sink ratio failed to recover the ovule blockage phenotype (Fig. 5). Moreover, none of the CWIN-silenced transgenic plants exhibited induction of the C-starvation reporter genes in the floral buds at stages 8 to 10, when ovules initiate (Fig. 6). These data show that the transgenic plants did not suffer from C starvation. Second, Suc unloading from the gynoecia SE/CC to ovule primordia follows a symplasmic pathway through interconnecting PD in Arabidopsis (Werner et al., 2011), and the amount of Suc required for ovule initiation would be very small in comparison with that for seed or fruit development (Palmer et al., 2015). Thus, CWIN is likely not a major player in delivering Suc as a C nutrient for ovule initiation. We therefore conclude that the essential and positive role exerted by CWIN for ovule development (Figs. 3 and 4) must be achieved through a signaling effect rather than provision of nutrients.

Plasma Membrane HXTs and RLKs May Sense and Transmit CWIN-Mediated Sugar Signaling for Ovule Initiation

Given that CWIN is a Suc-splitting enzyme functioning in the apoplasm, it is likely that any CWIN-induced changes in sugar concentration or flux would be sensed by and transmitted through plasma membrane proteins of the adjoining cells. In agreement with this prediction, a group of HXTs from the *SWEET* and *STP* family were downregulated in the *pSTK::* amiR*CWIN24* plants relative to the wild type (Table 3). Among the HXTs examined, transcripts of two representatives, *SWEET8* and *STP9*, were spatially colocalized with *CWIN2* and *CWIN4* during ovule initiation. Interestingly, although there are four Suc/H^+ symporters and six clade III *SWEET*s for Suc also expressed in the wild-type floral buds, none showed changes in transcript levels in the transgenic plants (Supplemental Table S3). These data suggest that CWIN-mediated sugar signaling may be transmitted by plasma membrane HXTs, but not by Suc transporters, from the cell wall matrix into the cytosol for ovule development. Alternatively, the alteration in extracellular sugar dynamics may be perceived by membrane RLKs. To this end, 28 DEGs encoding RLKs were differentially expressed in the CWIN-silenced plants (Table 3). RLKs, a group of transmembrane proteins, have been recognized as sensory proteins, functioning in a wide range of signal perception and transduction activities in plants (Wu et al., 2016). Significantly, 8 of the 23 upregulated RLKs among the transgenic plants, all of which belong to the leucine-rich repeat (LRR)-RLKs, were confirmed to be expressed in floral buds, including ovules, based on promoter::GUS analyses (Wu et al., 2016; Table 3). Collectively, the data suggest that these LRR-RLKs may be involved in CWIN-mediated ovule initiation and probably function as sensors to sense extracellular sugar levels or fluxes.

It is noted that genes encoding constituents of the RLK-mediated intracellular signaling pathway, Rop signaling, were also differentially expressed in response to CWIN silencing. As listed in Table 3, among those 15 small GTPase-related genes, the five genes involved in the Rop signaling pathway were all downregulated. These include two Rop genes and one Rop regulatory protein, ROPGEF9. There is evidence that LRR-RLK either phosphorylates RopGEF to activate Rop signaling to promoter pollen growth (Miyawaki and Yang, 2014) or activates Rop signaling upon sensing auxin to promote the development of pavement cells in leaf epidermis (Xu et al., 2014) and root hair elongation in Arabidopsis (Duan et al., 2010). It will be of significance to examine whether the CWIN-responsive RLKs identified in this study (Table 3) may transmit extracellular sugar signals into intracellular space in a similar manner.

Apart from a large number of LRR-RLKs, *WAK1* and *WAK2*, encoding a different class of RLKs, were also upregulated in response to CWIN silencing (Table 3). A *wak2* knockout mutant exhibited a reduced mRNA level and activity of vacuolar INV in the root that led to arrested growth on Suc-deficient medium, thus

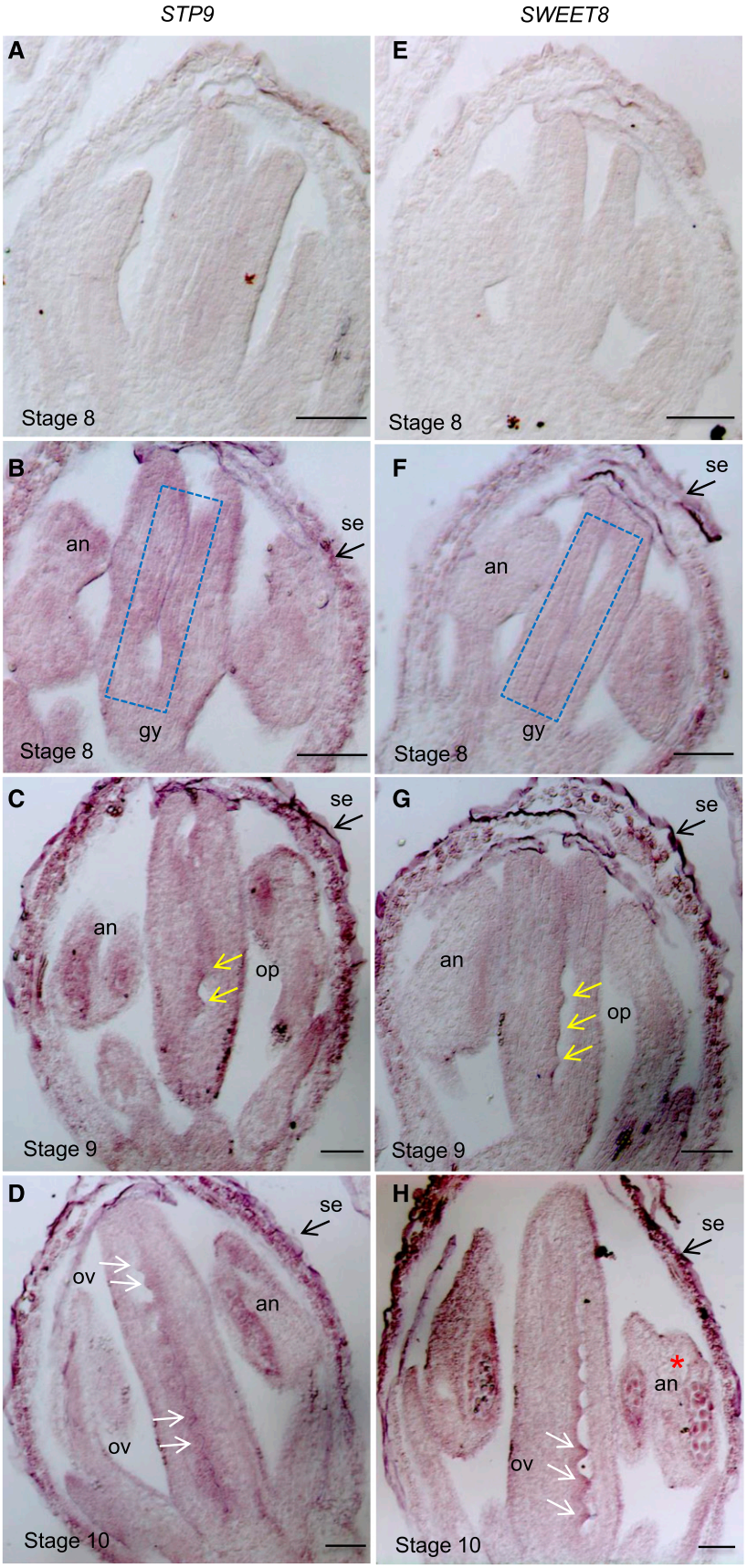

Figure 9. In situ hybridization analysis of *STP9* and *SWEET8* mRNA at the early stage of floral buds from stages 8 to 10 in wild-type (Col-0) Arabidopsis. A and E, In situ hybridization with a sense probe of *STP9* and *SWEET8* at stage 8 as controls. B to D, Sections of floral buds at stages 8 (B), 9 (C), and 10 (D) hybridized with the *STP9* antisense probe. Note the *STP9* mRNA signal detected in the middle part of the gynoecium, before ovule primordium initiation at stage 8 (dashed rectangle in B), and initiating ovule primordia (op) at stage 9 (yellow arrow; C), as well as the developing ovule (ov) at stage 10 (white arrow; D). The transcripts were also detected in anther (an) and sepals (se) across all the floral bud stages from 8 to 10. F to H, Sections of floral buds at stages 8 (F), 9 (G), and 10 (H) hybridized with the *SWEET8* antisense probe, showing *SWEET8* mRNA signals in the middle part of the gynoecium, before op initiation at stage 8 (dashed rectangle; F), and initiating op at stage 9 (yellow arrows; G), as well as the developing ovule at stage 10 (white arrows; H). The transcripts were also observed in an and se across all the floral bud stages from 8 to 10, similar to that of *STP9*. Note that the *SWEET8* signals were most evident in the developing ov (white arrow) and the an (red asterisk) containing developing microspores or male gametophytes (Sanders et al., 1999) at stage 10 (H). Floral stages 8 to 10 correspond to stages prior to (8), during (9), and after (10) ovule initiation, respectively (Smyth et al., 1990). Scale bars = 200 μm.

establishing a link between WAK and sugar signaling or metabolism (Kohorn et al., 2006). Our finding that silencing CWIN resulted in the upregulation of *WAK1* and *WAK2* indicates that expression of WAK genes themselves is subject to dynamics in extracellular sugar signaling. The extracellular domain of WAK is known to bind a polysacharride, pectin (Kohorn et al., 2006). It will be of significance to test whether WAK binds Suc or hexose. If it does, it could open up a new direction to determine the mechanism by which CWINs relay extracellular signaling to intracellular compartments.

Surprisingly, a group of aquaporins including four plasma membrane intrinsic proteins (PIPs) and two tonoplast intrinsic protein (TIPs) was downregulated in the CWIN-silenced transgenic plants (Table 3). It is unknown how dynamics in sugar metabolism signaling may regulate aquaporin gene expression. At the protein level, supplying Suc to C-starved Arabidopsis seedlings induced phosphorylation of aquaporins at their C terminus, promoting pore opening (Niittylä et al., 2007), possibly through SIRK1, a RLK, upon interaction with two other kinases containing extracellular domains, QSK1 and QSK2 (Wu et al., 2019). Physiologically, the reduced PIP and TIP expression in response to CWIN silencing could disrupt water influx to the initiating ovules, contributing to their abortion.

CWIN-Mediated Signaling May Be Relayed Ultimately through Early Auxin Response Genes and MADS TFs to Regulate Ovule Formation

RNA-seq analyses also revealed that over half (26 of 49) of the hormone-related DEGs were involved in auxin signaling, with most of these (19 of 26) being early auxin response genes, including 14 *SAUR*s, 4 *AUX/IAA*s, and 1 *GH3* (Table 1). This indicates that the early auxin response genes, especially *SAUR*s, may be closely

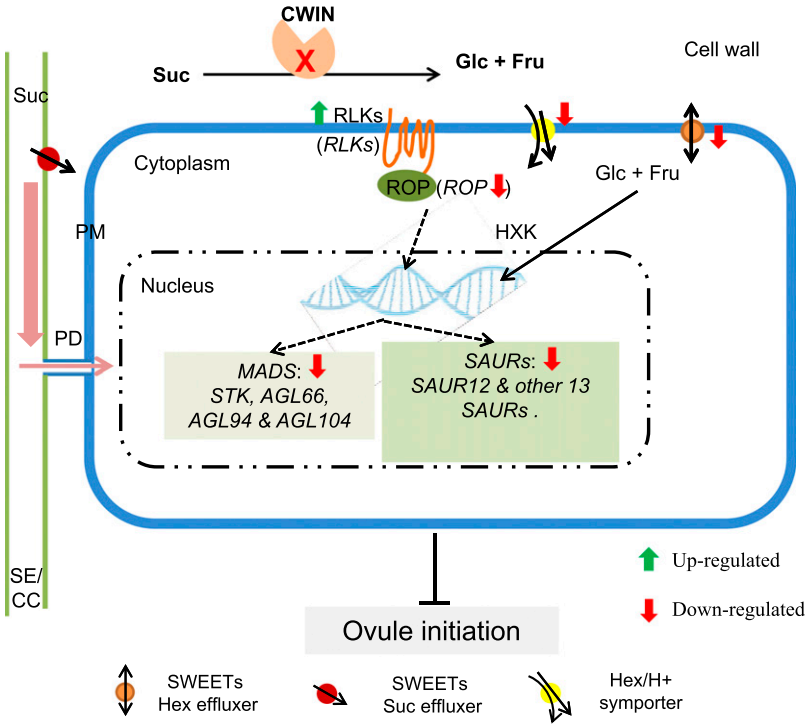

Figure 10. A model of how CWIN-mediated extracellular sugar signaling may be sensed at the plasma membrane and transduced to the intracellular space to modulate downstream pathways to regulate ovule initiation. In Arabidopsis gynoecia, Suc is unloaded symplasmically through PD for ovule primordium formation. Some Suc must have escaped to the cell wall for hydrolysis by CWIN into Glc and Fru. Silencing of CWIN would result in changes in the extracellular sugar level or flux, thereby generating sugar signal, which may be sensed by (1) RLKs transmitted through a small GTPase (Rop) into the cytoplasm that regulate gene expression in the nucleus and (2) HXTs, including clade I and II SWEETs and H^+/Hex symporters, to control cytosolic hexose level and sugar homeostasis, which may then be sensed by hexokinase or other proteins to regulate downstream gene expression. In this study, the expression of CWIN gene was silenced in the ovule initiating region. This genetic intervention reduced the expression of hexose/H^+ symporters and SWEETs for hexoses and likely their activities, thereby affecting intracellular sugar homeostasis and signaling. In parallel, expression of RLKs and Rops was increased and decreased, respectively, in response to CWIN silencing, suggesting a disturbance of the RLK-Rop-mediated signaling pathway. Both scenarios could disrupt downstream molecular pathways required for ovule initiation, including genes encoding MADS TFs, such as *STK*, and the early auxin signaling proteins, SAURs, leading to blockage of ovule initiation. Solid and dash-dotted lines indicate known and predicted pathways, respectively.

involved in CWIN-mediated ovule initiation. Relevant to this point, SAUR16 has been shown to positively regulate ovule number in Arabidopsis (van Mourik et al., 2017). SAUR16 shares 93% protein sequence similarity with one of the *SAUR*s, *SAUR12*, identified in our DEGs (Table 1) suggesting that *SAUR12* may function similarly to *SAUR16* in controlling ovule number.

Apart from 14 *SAUR*s, four *AUX/IAA* genes were also downregulated in the CWIN-silenced plants (Table 1). AUX/IAA is an essential component of the auxin signaling pathway, in which it functions as a repressor against auxin-inducible gene expression (Lau et al., 2008). Disruption of the AUX/IAA signaling pathway changes auxin signaling and homeostasis, and impairs cell division and root development (Vanneste et al., 2005; Yan et al., 2013). These findings, together with the importance of auxin for organogenesis such as lateral root initiation (Benková et al., 2003) and ovule formation (Galbiati et al., 2013), suggest that suppression of *AUX/IAA* in the CWIN-silenced transgenic plants may disrupt auxin signaling at the site of ovule initiation, resulting in blockage of ovule initiation. In this context, Glc could transcriptionally regulate 62% of IAA-related genes in Arabidopsis seedlings, including those involved in auxin signaling, such as *SAUR*, *AUX/IAA*, and *GH3* (Mishra et al., 2009). Together, the analyses indicate that the regulation of CWIN-mediated sugar signaling in ovule initiation may be achieved in part through auxin signaling genes such as *SAUR*s and *AUX/IAA*s.

It is unclear how downregulation of *SAUR*s could lead to inhibition of ovule development. An increasing number of studies indicate that *SAUR*s positively regulate cell expansion (Chae et al., 2012; Spartz et al., 2012), for example by repressing PP2C.D phosphatases, the D clade subfamily of type 2C protein phosphatases, to activate plasma membrane H^+-ATPases (Spartz et al., 2014). Plasma membrane H^+-ATPases pump protons to the apoplast (Hager, 2003), which is essential to maintaining cellular function for cell division and expansion characteristic of ovule initiation. These observations, together with the finding that two H^+-ATPase genes also were downregulated in the CWIN-silenced plants (Table 3), suggest that SAURs may contribute to ovule formation through positive effects on H^+-ATPase.

In addition to the auxin-related genes, a group of MADS-box TF genes including *STK* (formerly *AGL11*), *AGL66*, *AGL94*, and *AGL104* were downregulated in transgenic plants (Table 2). Many MADs TFs, such as AG, SHP1, and SHP2, function in ovule development (Skinner et al., 2004). Indeed, STK, which is phylogenetically close to AG and a homolog of SHP1 and SHP2, has been proven to be critical for establishment of ovule identity and development (Pinyopich et al., 2003). Although there is a lack of functional analysis for the other three MADS TFs in ovule development, expression-pattern and phylogeny analyses indicate that *AGL66*, *AGL94*, and *AGL104* may also be involved in CWIN-mediated ovule initiation. For example, the *AGL104* transcript was detected in the placenta and ovule primordia (Pařenicová et al., 2003), and *AGL66* and *AGL94* share a monophyletic clade with *AGL104* (Smaczniak et al., 2012). To test whether those differentially expressed MADS TF genes were involved in CWIN-mediated ovule development, *STK* was overexpressed in the transgenic background, which led to partial complementation of the ovule phenotype in the CWIN-silenced plants (Fig. 6), pointing to *STK* as a downstream target of the CWIN-mediated ovule initiation pathway. It remains to be established s how CWIN-mediated sugar signaling could regulate *STK* expression. Nevertheless, sequence analyses using the AtcisDB tool (http://arabidospis .med.ohio-state.ed/AticDB/) identified three ARF1 binding sites (TGTCTC) in the *STK* promoter (approximately −1,261 to 1,266, approximately −2,058 to −2,063, and approximately −3,292 to 3,297). The altered expression of auxin signaling genes (*SAUR*s and *AUX/IAA*s) observed in the CWIN-silenced floral buds (see above in this section; Table 1) may disrupt the binding of ARF1 with the *STK* promoter for its transcription, leading to the reduction of *STK* transcript, a possible focus for future studies.

A Model of CWIN-Mediated Ovule Development through Sugar Signaling

Based on the above analysis, we propose a model of how CWIN may regulate ovule development (Fig. 10). Sugar signals generated by CWIN in the cell wall matrix may be sensed by and transmitted through plasma membrane-localized HXTs, to modulate cytosolic sugar homeostasis and sugar signaling, and/or RLKs, to potentially interact with small GTPase (Rop) pathways in the cytoplasm. The CWIN-originated signals are then relayed to the nuclei to regulate expression of genes encoding auxin signaling components and MADS-box TFs, thereby modulating ovule initiation and differentiation. The model provides directions for future studies to determine the identity and transmission pathways of the sugar signals generated by CWIN for ovule development.

MATERIALS AND METHODS

Plant Materials and Growth Condition

Arabidopsis (*Arabidopsis thaliana*) ecotype Columbia-0 (Col-0) and the transgenic plants generated from this background were grown in growth cabinets under long-day condition (16 h light at 22°C and 8 h dark at 18°C, with illumination at 120–150 μmol s^{-1} m^{-2} and 60% to 70% relative humidity).

in Situ Hybridization

In situ hybridization was carried out using our established protocol (Jin et al., 2009; Wang and Ruan, 2012) with minor modifications in sample fixation, where Arabidopsis inflorescences were fixed in formaldehyde-acetic acid fixative containing 50% (v/v) ethanol, 5% (v/v) glacial acetic acid, and 3.7% (v/v) formaldehyde at 4°C overnight. To generate gene specific probes, the most

diverse sequences at the 3′ untranslated region (3′ UTR) were selected for probe synthesis. For *CWIN2*, a 139-bp *CWIN2* fragment ranging from 50 to 189 bp downstream of the stop codon, was amplified using *CWIN2*-3′ UTR in situ primers, whereas a 134-bp fragment, ranging from 27 to 161 bp downstream of the stop codon of *CWIN4*, was amplified using *CWIN4*-3′ UTR in situ primers for *CWIN4* probe synthesis. Similarly, specific fragments for two HXTs (*STP9* and *SWEET8*) were cloned from their corresponding 3′ UTR region and synthesized using their respective 3′ UTR in situ primers. All primers are listed in Supplemental Table S4. These fragments were cloned into the pGEM-T easy vector with *Bam*HI and *Xba*I restriction enzymes and transcribed for synthesis of sense and antisense RNA probes using T7 and SP6 RNA polymerases (Roche Diagnostics), respectively, labeled with digoxigenin-UTP (Roche Diagnostics).

RNA Extraction and RT-qPCR

Total RNA was extracted from a pooled sample of flower buds at stages 8 to 10, when the ovule initiates (Smyth et al., 1990), using TRIzol Reagent (Invitrogen) according to the manufacturer's instructions. About 1 μg of RNA was treated with DNase (Promega) to remove the residual genomic DNA. DNase treated-RNA was reversely transcribed into complementary DNA (cDNA) using the SuperScript III system (Invitrogen) along with 50 μ M oligo(dT)$_{20}$ and 10 μM deoxynucleoside triphosphate according to the manufacturer's protocol.

RT-qPCR was performed with SYBR Green fluorescent dye (Invitrogen) and Platinum *Taq* DNA polymerase (Invitrogen) on a Rotor-gene Q instrument (Qiagen). Gene-specific primers used in this study are listed in Supplemental Table S5. The relative expression level (R) of each target gene is calculated based on the Pfaffl method (Pfaffl, 2001):

$$R = \frac{\left(E_{\text{target}}\right)^{\Delta \text{Ct, target (calibrator test)}}}{\left(E_{\text{ref}}\right)^{\Delta \text{Ct, ref (calibrator test)}}}$$

In the above equation, E_{target} and $E_{\text{ref (reference)}}$ are amplification efficiencies of the target and reference genes, respectively; ΔCt, target (calibrator test) is the cycle threshold (Ct) of the target gene in the calibrator minus the Ct of the target gene in the test sample; and ΔCt, ref (calibrator test) is the Ct of the reference gene in the calibrator minus the Ct of reference gene in the test sample. Among the four Arabidopsis reference genes, namely the F-box protein gene *FBX* (At5g15710), polyubiquitin gene *UBC21* (At5g25760), *UBC9* (At4g27960), and the PP2A catalytic subunit gene *PP2A* (At1g13320), *FBX* and *UBC21* showed the most stable expression among wild-type and transgenic cDNA samples based on analysis using geNORM software (http://medgen.ugent.be/jvdesomp/genorm/). Therefore, these two genes were used as reference genes for qPCR analyses in this study.

Invertase Enzyme Assay

Gynoecia-enriched tissues were dissected out from the sample pool of flower buds at stages 8 to 10 for activity assay of CWIN, VIN, and CIN as previously described (Tomlinson et al., 2004).

Design and Synthesis of amiRNA against *CWIN2* and *CWIN4*

Taking advantage of the high specificity conferred by amiRNA silencing technology (Tiwari et al., 2014), we designed amiRNA*CWIN24*, which targeted a 21-nucleotide (nt) sequence, conserved in *CWIN2* and *CWIN4* but not in *CWIN1* and *CWIN5* (Supplemental Fig. S3A), upstream of the CWIN catalytic domain (WECPD; Supplemental Fig. S3B) to achieve a maximal silencing effect against CWIN functionality. The amiRNA*CWIN24* was chosen based on the selection rules for the amiRNA-target sequence (Eamens et al., 2014) to target a "shared" 21-nt sequence conserved between *CWIN2* and *CWIN4* from 278 to 299 bp downstream of the start codon ATG (Supplemental Fig. S3, A and B). The approach of amiRNA-mediated gene silencing exploits the intrinsic nature of the miRNA biogenesis pathway. Replacement of the miRNA/miRNA* sequence of endogenous presynthesized amiRNA precursor (premiRNA) with amiRNA/amiRNA* while maintaining the double-strand RNA hairpin stem-loop structure can generate mature amiRNAs by key enzymes recruited for biogenesis of endogenous miRNA (Tiwari et al., 2014). Here, the endogenous miRNA159B biogenesis pathway was exploited, since miRNA159B is highly accumulated in floral tissues (Allen et al., 2007). We replaced the miRNA159B/miRNA159B* (guide and passenger strand, respectively) of the endogenous premiRNA159B with amiRNA*CWIN24*/amiRNA*CWIN24** (Supplemental Fig. S3C). To mimic the premiRNA159B structure characterized with three mismatches at positions 12, 13, and 21 of the miRNA159B* passenger strand (Supplemental Fig. S3C), we introduced three mismatches at the same nucleotide positions of miRNA*CWIN24** passenger strand (Supplemental Fig. S3C). This ensures that the modified premiRNA*CWIN24* fragment is recognized and processed by the endogenous miRNA biogenesis pathway. The modified premiRNA*CWIN24* (Supplemental Fig. S3C) was synthesized (Integrated DNA Technologies) with sequence of preamiRNA*CWIN24* list in Supplemental Table S5.

Construction of *pSTK::amiRCWIN* and Its Transformation into Arabidopsis

To achieve specific silencing of *CWIN2* and *CWIN4* at the ovule initiation site, an ovule-specific *STK* promoter that comprised the region from 1.8 kb upstream to 1.1 kb downstream of the translation start codon and contained the first exon and intron was used to drive the expression of amiRNA*CWIN24*. The 2.9-kb *STK* promoter was cloned into the pART7rc vector using the primers listed in Supplemental Table S5. *SacI*, *NotI*, and *XhoI* restriction sites were added to its 5′ and 3′ ends, respectively. The *pSTK* was introduced into vector pART7rc by replacing the CaMV 35S promoter with restriction sites *SacI* and *XhoI*. Subsequently, the 258-bp presynthesized amiRNA precursor (preamiRNA*CWIN24*) was cloned into the *pSTK*-ART7 vector with *Eco*RI and *Xba*I to form the *pSTK*-amiRC*WIN*-ART7rc vector. The gene cassette *pSTK*-amiRC*WIN24* was released by digestion with *Not*I, which was then cloned into the binary vector pBARTrc. To complement the reduction of *STK* expression in the *pSTK*-amiRC*WIN24* transgenic plants, a complementary vector *pSTK-STK*(CDS)-pCAMBIA1300 was constructed to drive the expression of a 771-bp *STK* CDS.

Arabidopsis inflorescences were dipped in cell suspension of the *Agrobacterium tumefaciens* strain AGL-1 (Zhang et al., 2006), which carried the target binary vector, for 10 s with gentle agitation. Dipped plants were removed from cell suspension and drained for 3 to 5 s and were then covered with plastic film to maintain high humidity for 16 to 24 h before being moved to a glasshouse for recovery and growth under normal conditions.

Ovule, Seed, and Silique Phenotyping

For ovule phenotyping, flower buds at stages 10 to 11 (~2 to 1 d before flowering; Roeder and Yanofsky, 2006) were collected and fixed in ethanol/acetic acid (9:1) overnight, and then washed by 90% (v/v) ethanol, followed by a further wash with 70% (v/v) ethanol after a 30-min interval. Thereafter, flower buds were mounted in a mixture of chloralhydrate/glycerol/water (8:1:2 [v/v/v]) and cleared overnight. Cleared flower buds were dissected to expose the gynoecium and observed under differential interference contrast with a Leica dissection microscope. For analyses of seed number and silique length, fully expanded siliques at stage 17 (~5 d after flowering; Roeder and Yanofsky, 2006) were collected from the main inflorescences of each genotype. These siliques were cleared and mounted as described (Berleth and Jurgens, 1993). For seed number counting, siliques were fixed and clear mounted using the same method as for ovule phenotyping.

RNA Isolation and Illumina Sequencing

A pooled sample of flower buds was harvested at stages 8 to 10, which covers stages prior to (stage 8), during (stage 9), and after (stage 10) ovule initiation. RNA was extracted from the pooled sample of the wild type and transgenic line 4-3, which exhibits the most severe reduction in ovule number, using the Qiagen RNA Plant Mini Kit, followed by an on-column DNase treatment to eliminate genome DNA by DNaseI digestion. Eight RNA extracts (four biological replicates for each of two genotypes), each containing at least 5 μg of total RNA, were sent to the Australia Genome Research Facility (AGRF) for RNA sequencing. RNA quality was determined by Agilent 2100 Bioanalyzer, and only samples with RNA integrity number >8 were further processed for cDNA library preparation and sequencing. Sequencing of the cDNA libraries was performed using an Illumina Hiseq2500 with 125-bp pair end with an average sequencing depth of 30 million reads.

Sequencing Trimming and Mapping and Determination of DEGs

Raw reads were trimmed using CLC Genomics Workbench 10.1.1 (Qiagen) based on Ru et al. (2017) with some modifications. Briefly, raw reads were

trimmed as follows: (1) Removal of reads with quality scores <20 (base-calling error probability <0.01) and those with more than two ambiguous nucleotides; (2) adapter trimming; and (3) removal of reads with sequence length of <15 nucleotides. To estimate gene expression level, trimmed reads were mapped to the Arabidopsis reference genome sequence (TAIR10) using the CLC Genomics Workbench, which allows unique mapping with a maximum of two mismatches. Reads mapped to unigenes were counted and used for expression analysis. The number of mapped reads per kilobase per million reads (RPKM) was used as a measure of the expression level of each gene. Using the CLC genomic RNA-seq differential analysis tool, DEGs of transgenic samples, as compared to wild-type samples, were identified based on the following criteria: (1) mean RPKM value ≥1 in at least one sample, in either the wild-type or transgenic group, where only genes exhibiting a mean RPKM ≥1 were considered to be expressed; (2) false discovery rate <0.05; and (3) log2 FC >1 or less than −1. MAPMAN (Thimm et al., 2004) was used to identify functional categories of the DEGs. The RNA-seq data have been uploaded to the National Center for Biotechnological Information web site (https://www.ncbi.nlm.nih.gov/geo/; with data accession no. GSE139917).

Statistical Analysis

CLC Genomics Workbench 10.1.1 (Qiagen) was used for PCA of RNA-seq data. One-way ANOVA was performed for data analyses using JMP 11 software. For details, see figure legends and table captions.

Accession Numbers

Sequence data from this article can be found in the GenBank/EMBL data libraries under the accession numbers listed in Supplemental Tables S2 to S5. RNA-seq data can be accessed through the Gene Expression Omnibus portal of GenBank with accession number GSE139917.

Supplemental Data

The following supplemental materials are available.

Supplemental Figure S1. Statistical analysis of silique length and seed number of five T3 homozygous *pSTK-amiRNACWIN24* transgenic lines compared with wild-type plants.

Supplemental Figure S2. Overall assessment of the quality of RNA-seq data between wild-type plants and *pSTK-amiRNACWIN24* transgenic lines (4-3).

Supplemental Figure S3. Custom design of amiRCWIN24.

Supplemental Table S1. Blockage of ovule initiation in *pSTK*-amiRNA*CWIN24* transgenic plants compared with the wild type

Supplemental Table S2. A total of 1,490 genes differentially expressed in the *pSTK*-amiRNACWIN24 transgenic floral buds at stages 8 to 10 compared with the wild type

Supplemental Table S3. A total of 76 TF genes differentially expressed in stage-8 to stage-10 floral buds of *pSTK*::amiRNACWIN24 transgenic plants compared with the wild type

Supplemental Table S4. *STP* genes detectable in floral buds during ovule initiation in both wild-type and *pSTK-amiRNACWIN24* transgenic plants, including DEGs and non-DEGs

Supplemental Table S5. All oligos used in this study

ACKNOWLEDGMENTS

The authors greatly appreciate Dr, Andy Eamens for his advice on the design of artificial microRNA construct. S.J.L. gratefully acknowledges support from the University of Newcastle for providing a postgraduate scholarship.

Received April 3, 2020; accepted April 13, 2020; published April 24, 2020.

LITERATURE CITED

Allen RS, Li J, Stahle MI, Dubroué A, Gubler F, Millar AA (2007) Genetic analysis reveals functional redundancy and the major target genes of the *Arabidopsis* miR159 family. Proc Natl Acad Sci USA **104:** 16371–16376

Benková E, Michniewicz M, Sauer M, Teichmann T, Seifertová D, Jürgens G, Friml J (2003) Local, efflux-dependent auxin gradients as a common module for plant organ formation. Cell **115:** 591–602

Berleth T, Jurgens G (1993) The role of the *monopteros* gene in organising the basal body region of the *Arabidopsis* embryo. Development **118:** 575–587

Braun DM, Wang L, Ruan Y-L (2014) Understanding and manipulating sucrose phloem loading, unloading, metabolism, and signalling to enhance crop yield and food security. J Exp Bot **65:** 1713–1735

Büttner M (2010) The *Arabidopsis* sugar transporter (AtSTP) family: An update. Plant Biol (Stuttg) **12**(Suppl 1): 35–41

Chae K, Isaacs CG, Reeves PH, Maloney GS, Muday GK, Nagpal P, Reed JW (2012) Arabidopsis SMALL AUXIN UP RNA63 promotes hypocotyl and stamen filament elongation. Plant J **71:** 684–697

Cheng W-H, Chourey PS (1999) Genetic evidence that invertase-mediated release of hexoses is critical for appropriate carbon partitioning and normal seed development in maize. Theor Appl Genet **98:** 485–495

Cucinotta M, Colombo L, Roig-Villanova I (2014) Ovule development, a new model for lateral organ formation. Front Plant Sci **5:** 117

Duan Q, Kita D, Li C, Cheung AY, Wu H-M (2010) FERONIA receptor-like kinase regulates RHO GTPase signaling of root hair development. Proc Natl Acad Sci USA **107:** 17821–17826

Eamens AL, McHale M, Waterhouse PM (2014) The use of artificial microRNA technology to control gene expression in *Arabidopsis thaliana*. *In* JJ Sanchez-Serrano, J Salinas, eds, Arabidopsis Protocols, Methods in Molecular Biology, volume 1062. Humana Press, Totowa, NJ, pp 211–224

Ebel C, Mariconti L, Gruissem W (2004) Plant retinoblastoma homologues control nuclear proliferation in the female gametophyte. Nature **429:** 776–780

Eom J-S, Chen L-Q, Sosso D, Julius BT, Lin IW, Qu X-Q, Braun DM, Frommer WB (2015) SWEETs, transporters for intracellular and intercellular sugar translocation. Curr Opin Plant Biol **25:** 53–62

Galbiati F, Sinha Roy D, Simonini S, Cucinotta M, Ceccato L, Cuesta C, Simaskova M, Benkova E, Kamiuchi Y, Aida M, et al (2013) An integrative model of the control of ovule primordia formation. Plant J **76:** 446–455

Griffith M, Griffith OL, Mwenifumbo J, Goya R, Morrissy AS, Morin RD, Corbett R, Tang MJ, Hou Y-C, Pugh TJ, et al (2010) Alternative expression analysis by RNA sequencing. Nat Methods **7:** 843–847

Hager A (2003) Role of the plasma membrane H^+-ATPase in auxin-induced elongation growth: Historical and new aspects. J Plant Res **116:** 483–505

Hayashi K (2012) The interaction and integration of auxin signaling components. Plant Cell Physiol **53:** 965–975

Heyer AG, Raap M, Schroeer B, Marty B, Willmitzer L (2004) Cell wall invertase expression at the apical meristem alters floral, architectural, and reproductive traits in *Arabidopsis thaliana*. Plant J **39:** 161–169

Jin J, Tian F, Yang D-C, Meng Y-Q, Kong L, Luo J, Gao G (2017) PlantTFDB 4.0: Toward a central hub for transcription factors and regulatory interactions in plants. Nucleic Acids Res **45**(D1): D1040–D1045

Jin Y, Ni D-A, Ruan Y-L (2009) Posttranslational elevation of cell wall invertase activity by silencing its inhibitor in tomato delays leaf senescence and increases seed weight and fruit hexose level. Plant Cell **21:** 2072–2089

Kohorn BD, Kobayashi M, Johansen S, Riese J, Huang L-F, Koch K, Fu S, Dotson A, Byers N (2006) An Arabidopsis cell wall-associated kinase required for invertase activity and cell growth. Plant J **46:** 307–316

Kooiker M, Airoldi CA, Losa A, Manzotti PS, Finzi L, Kater MM, Colombo L (2005) BASIC PENTACYSTEINE1, a GA binding protein that induces conformational changes in the regulatory region of the homeotic *Arabidopsis* gene *SEEDSTICK*. Plant Cell **17:** 722–729

Lau S, Jürgens G, De Smet I (2008) The evolving complexity of the auxin pathway. Plant Cell **20:** 1738–1746

Lauxmann MA, Annunziata MG, Brunoud G, Wahl V, Koczut A, Burgos A, Olas JJ, Maximova E, Abel C, Schlereth A, et al (2016) Reproductive failure in *Arabidopsis thaliana* under transient carbohydrate limitation: Flowers and very young siliques are jettisoned and the meristem is maintained to allow successful resumption of reproductive growth. Plant Cell Environ **39:** 745–767

León P, Sheen J (2003) Sugar and hormone connections. Trends Plant Sci **8:** 110–116

Li J, Wu L, Foster R, Ruan Y-L (2017) Molecular regulation of sucrose catabolism and sugar transport for development, defence and phloem function. J Integr Plant Biol **59:** 322–335

Liu Y-H, Offler CE, Ruan Y-L (2016) Cell wall invertase promotes fruit set under heat stress by suppressing ROS-independent cell death. Plant Physiol **172:** 163–180

Ludwig-Müller J (2011) Auxin conjugates: Their role for plant development and in the evolution of land plants. J Exp Bot **62:** 1757–1773

Miller ME, Chourey PS (1992) The maize invertase-deficient miniature-1 seed mutation is associated with aberrant pedicel and endosperm development. Plant Cell **4:** 297–305

Mishra BS, Singh M, Aggrawal P, Laxmi A (2009) Glucose and auxin signaling interaction in controlling *Arabidopsis thaliana* seedling root growth and development. PLoS One **4:** e4502

Miyawaki KN, Yang Z (2014) Extracellular signals and receptor-like kinases regulating ROP GTPases in plants. Front Plant Sci **5:** 449

Niittylä T, Fuglsang AT, Palmgren MG, Frommer WB, Schulze WX (2007) Temporal analysis of sucrose-induced phosphorylation changes in plasma membrane proteins of *Arabidopsis*. Mol Cell Proteomics **6:** 1711–1726

Palmer WM, Ru L, Jin Y, Patrick JW, Ruan Y-L (2015) Tomato ovary-to-fruit transition is characterized by a spatial shift of mRNAs for cell wall invertase and its inhibitor with the encoded proteins localized to sieve elements. Mol Plant **8:** 315–328

Pařenicová L, de Folter S, Kieffer M, Horner DS, Favalli C, Busscher J, Cook HE, Ingram RM, Kater MM, Davies B, et al (2003) Molecular and phylogenetic analyses of the complete MADS-Box transcription factor family in *Arabidopsis*: New openings to the MADS world. Plant Cell **15:** 1538–1551

Patrick JW (1997) Phloem unloading: Sieve element unloading and post-sieve element transport. Annu Rev Plant Physiol Plant Mol Biol **48:** 191–222

Pfaffl MW (2001) A new mathematical model for relative quantification in real-time RT-PCR. Nucleic Acids Res **29:** e45

Pinyopich A, Ditta GS, Savidge B, Liljegren SJ, Baumann E, Wisman E, Yanofsky MF (2003) Assessing the redundancy of MADS-box genes during carpel and ovule development. Nature **424:** 85–88

Ren H, Gray WM (2015) SAUR proteins as effectors of hormonal and environmental signals in plant growth. Mol Plant **8:** 1153–1164

Roeder AHK, Yanofsky MF (2006) Fruit development in *Arabidopsis*. The Arabidopsis Book **4:** e0075

Roitsch T, González M-C (2004) Function and regulation of plant invertases: Sweet sensations. Trends Plant Sci **9:** 606–613

Ru L, Osorio S, Wang L, Fernie AR, Patrick JW, Ruan Y-L (2017) Transcriptomic and metabolomics responses to elevated cell wall invertase activity during tomato fruit set. J Exp Bot **68:** 4263–4279

Ruan Y-L (2012) Signaling role of sucrose metabolism in development. Mol Plant **5:** 763–765

Ruan Y-L (2014) Sucrose metabolism: Gateway to diverse carbon use and sugar signaling. Annu Rev Plant Biol **65:** 33–67

Ruan YL, Jin Y, Yang YJ, Li GJ, Boyer JS (2010) Sugar input, metabolism, and signaling mediated by invertase: Roles in development, yield potential, and response to drought and heat. Mol Plant **3:** 942–955

Sanders PM, Bui AQ, Weterings K, McIntire KN, Hsu Y-C, Lee PY, Truong MT, Beals TP, Goldberg RB (1999) Anther developmental defects in *Arabidopsis thaliana* male-sterile mutants. Sex Plant Reprod **11:** 297–322

Schmid M, Davison TS, Henz SR, Pape UJ, Demar M, Vingron M, Schölkopf B, Weigel D, Lohmann JU (2005) A gene expression map of *Arabidopsis thaliana* development. Nat Genet **37:** 501–506

Skinner DJ, Hill TA, Gasser CS (2004) Regulation of ovule development. Plant Cell **16**(Suppl): S32–S45

Smaczniak C, Immink RGH, Angenent GC, Kaufmann K (2012) Developmental and evolutionary diversity of plant MADS-domain factors: Insights from recent studies. Development **139:** 3081–3098

Smyth DR, Bowman JL, Meyerowitz EM (1990) Early flower development in *Arabidopsis*. Plant Cell **2:** 755–767

Spartz AK, Ren H, Park MY, Grandt KN, Lee SH, Murphy AS, Sussman MR, Overvoorde PJ, Gray WM (2014) SAUR inhibition of PP2C-D phosphatases activates plasma membrane H^+-ATPases to promote cell expansion in *Arabidopsis*. Plant Cell **26:** 2129–2142

Spartz AK, Lee SH, Wenger JP, Gonzalez N, Itoh H, Inzé D, Peer WA, Murphy AS, Overvoorde PJ, Gray WM (2012) The *SAUR19* subfamily of *SMALL AUXIN UP RNA* genes promote cell expansion. Plant J **70:** 978–990

Sturm A (1999) Invertases. Primary structures, functions, and roles in plant development and sucrose partitioning. Plant Physiol **121:** 1–8

Thimm O, Bläsing O, Gibon Y, Nagel A, Meyer S, Krüger P, Selbig J, Müller LA, Rhee SY, Stitt M (2004) MAPMAN: A user-driven tool to display genomics data sets onto diagrams of metabolic pathways and other biological processes. Plant J **37:** 914–939

Tiwari M, Sharma D, Trivedi PK (2014) Artificial microRNA mediated gene silencing in plants: Progress and perspectives. Plant Mol Biol **86:** 1–18

Tomlinson KL, McHugh S, Labbe H, Grainger JL, James LE, Pomeroy KM, Mullin JW, Miller SS, Dennis DT, Miki BLA (2004) Evidence that the hexose-to-sucrose ratio does not control the switch to storage product accumulation in oilseeds: Analysis of tobacco seed development and effects of overexpressing apoplastic invertase. J Exp Bot **55:** 2291–2303

van Mourik H, van Dijk ADJ, Stortenbeker N, Angenent GC, Bemer M (2017) Divergent regulation of Arabidopsis *SAUR* genes: A focus on the *SAUR10*-clade. BMC Plant Biol **17:** 245

Vanneste S, De Rybel B, Beemster GTS, Ljung K, De Smet I, Van Isterdael G, Naudts M, Iida R, Gruissem W, Tasaka M, et al (2005) Cell cycle progression in the pericycle is not sufficient for SOLITARY ROOT/IAA14-mediated lateral root initiation in *Arabidopsis thaliana*. Plant Cell **17:** 3035–3050

Vernoud V, Horton AC, Yang Z, Nielsen E (2003) Analysis of the small GTPase gene superfamily of Arabidopsis. Plant Physiol **131:** 1191–1208

Wan H, Wu L, Yang Y, Zhou G, Ruan Y-L (2018) Evolution of sucrose metabolism: The dichotomy of invertases and beyond. Trends Plant Sci **23:** 163–177

Wang E, Wang J, Zhu X, Hao W, Wang L, Li Q, Zhang L, He W, Lu B, Lin H, et al (2008) Control of rice grain-filling and yield by a gene with a potential signature of domestication. Nat Genet **40:** 1370–1374

Wang L, Ruan Y-L (2012) New insights into roles of cell wall invertase in early seed development revealed by comprehensive spatial and temporal expression patterns of *GhCWIN1* in cotton. Plant Physiol **160:** 777–787

Wang L, Ruan Y-L (2013) Regulation of cell division and expansion by sugar and auxin signaling. Front Plant Sci **4:** 163

Wang Z, Wei X, Yang J, Li H, Ma B, Zhang K, Zhang Y, Cheng L, Ma F, Li M (2019) Heterologous expression of the apple hexose transporter MdHT2.2 altered sugar concentration with increasing cell wall invertase activity in tomato fruit. Plant Biotechnol J **18:** 540–552

Weber H, Borisjuk L, Wobus U (1996) Controlling seed development and seed size in Vicia faba: A role for seed coat-associated invertases and carbohydrate state. Plant J **10:** 823–834

Weber H, Borisjuk L, Wobus U (2005) Molecular physiology of legume seed development. Annu Rev Plant Biol **56:** 253–279

Werner D, Gerlitz N, Stadler R (2011) A dual switch in phloem unloading during ovule development in *Arabidopsis*. Protoplasma **248:** 225–235

Weschke W, Panitz R, Gubatz S, Wang Q, Radchuk R, Weber H, Wobus U (2003) The role of invertases and hexose transporters in controlling sugar ratios in maternal and filial tissues of barley caryopses during early development. Plant J **33:** 395–411

Wu XN, Chu L, Xi L, Pertl-Obermeyer H, Li Z, Sklodowski K, Sanchez-Rodriguez C, Obermeyer G, Schulze WX (2019) Sucrose-Induced Receptor Kinase 1 is modulated by an interacting kinase with short extracellular domain. Mol Cell Proteomics **18:** 1556–1571

Wu Y, Xun Q, Guo Y, Zhang J, Cheng K, Shi T, He K, Hou S, Gou X, Li J (2016) Genome-wide expression pattern analyses of the *Arabidopsis* leucine-rich repeat receptor-like kinases. Mol Plant **9:** 289–300

Xu L, Zhu L, Tu L, Liu L, Yuan D, Jin L, Long L, Zhang X (2011) Lignin metabolism has a central role in the resistance of cotton to the wilt fungus *Verticillium dahliae* as revealed by RNA-seq-dependent transcriptional analysis and histochemistry. J Exp Bot **62:** 5607–5621

Xu T, Dai N, Chen J, Nagawa S, Cao M, Li H, Zhou Z, Chen X, De Rycke R, Rakusová H, et al (2014) Cell surface ABP1-TMK auxin-sensing complex activates ROP GTPase signaling. Science **343:** 1025–1028

Yan D-W, Wang J, Yuan T-T, Hong L-W, Gao X, Lu Y-T (2013) Perturbation of auxin homeostasis by overexpression of wild-type *IAA15* results in impaired stem cell differentiation and gravitropism in roots. PLoS One **8:** e58103

Zanor MI, Osorio S, Nunes-Nesi A, Carrari F, Lohse M, Usadel B, Kühn C, Bleiss W, Giavalisco P, Willmitzer L, et al (2009) RNA interference of LIN5 in tomato confirms its role in controlling Brix content, uncovers the influence of sugars on the levels of fruit hormones, and demonstrates the importance of sucrose cleavage for normal fruit development and fertility. Plant Physiol **150:** 1204–1218

Zhang X, Henriques R, Lin S-S, Niu Q-W, Chua N-H (2006) Agrobacterium-mediated transformation of *Arabidopsis thaliana* using the floral dip method. Nat Protoc **1:** 641–646